Measurement and modeling of denitrification in sand-bed streams of varying land use

A THESIS

SUBMITTED TO THE FACULTY OF THE GRADUATE SCHOOL

OF THE UNIVERSITY OF MINNESOTA

BY

Kristopher Steven Guentzel

IN PARTIAL FULFILLMENT OF THE REQUIREMENTS

FOR THE DEGREE OF

MASTER OF SCIENCE

Advisor: Dr. Miki Hondzo

February 2013

Abstract

Processes that govern transport and transformation of aquatic nitrogen (N) are of growing importance due to increases in anthropogenic N input from fertilizer application and fossil fuel combustion. Denitrification, the incremental reduction of soluble nitrate (NO_3) to gaseous end products, is the main pathway in which N is biologically removed from aquatic ecosystems. In this study denitrification is measured from sediment cores in 5 streams in central Minnesota, USA, using denitrification enzyme activity (DEA) assays as well as microbiological techniques including the amplification of nirS gene fragments through qPCR. Hydraulic and environmental variables are measured in the vicinity of the sediment cores to determine a possible mediating influence of fluid flow and chemical variables on denitrification activity. Denitrification rates measured using DEA analysis with amended nutrients ranged from 0.02-10.1 mg-N m^{-2} hr^{-1}. Denitrification rates measured without amended nutrients were a factor of 5.35 less on average and ranged from 0.03-0.98 mg-N m^{-2} hr^{-1}. The abundance of the denitrifier gene nirS was positively correlated with denitrification potential measurements ($R^2 = 0.79$, $P < 0.001$) for most of the streams studied. NirS distribution in one of the sites, a field scale experimental stream called the Outdoor StreamLab, followed the spatial distribution of benthic organic matter closely along the sediment bed and through the sediment column.

Predictive models to determine NO_3 uptake via denitrification were derived from hydraulic, morphologic and water quality variables. The first used hydraulic data collected over 3 summers in the Outdoor StreamLab. A Gaussian-type function was fit to these data and was dependent on fluid flow and channel characteristics within the stream system. The second model was derived following dimensional analysis on data from the Outdoor StreamLab and 4 other natural streams

of varying watershed and in-stream conditions. This predictive model integrated not only stream hydraulic data but also environmental, morphological and DEA measurements for nutrient-amended and unamended samples. The proposed model explained 75% and 60% of the variability in amended and unamended DEA rates, respectively. Results from this study verify that denitrification is ubiquitous across varying stream systems but is most dependent on the distribution of sediment organic matter and interstitial pore space as well as stream hydraulic characteristics.

Table of Contents

List of Tables

List of Figures

Notation

Nitrogen Species [units if used]

N	Nitrogen
N_2	Diatomic nitrogen or dinitrogen
NH_3	Ammonia [mg-N L^{-1}]
NH_4	Ammonium
NO_3	Nitrate [mg-N L^{-1}]
NO_2	Nitrite [mg-N L^{-1}]
NO	Nitric Oxide
N_2O	Nitrous Oxide [µg-N L^{-1}]
TDN	Total Dissolved Nitrogen [mg L^{-1}]

Environmental Variables [units if used]

AFDM	Ash-Free Dry Mass [g]
BOM	Benthic Organic Matter [g cm^{-2}]
C	Carbon
C_S	Near-bed NO_3 concentration [mg-N L^{-1}]
C_V	Vertically-averaged NO_3 concentration [mg-N L^{-1}]
C_V/C_S	Dimensionless NO_3 concentration [dimensionless]
C_{NO_3}	NO_3 concentration (vertically-averaged) used during dimensional analysis [mg-N L^{-1}]
DO	Dissolved Oxygen [% saturated]
DOC	Dissolved Organic Carbon [mg L^{-1}]
DR_A	Denitrification Rate for nutrient-amended conditions [mg-N m^{-2} hr^{-1}]

DR_U	Denitrification Rate for unamended (or ambient) conditions [mg-N m^{-2} hr^{-1}]
J_{NO_3}	Denitrification rate as determined by dimensional analysis [mg-N m^{-2} hr^{-1}]
SRP	Soluble Reactive Phosphorus [μg L^{-1}]
ρ_W	Water density [g cm^{-3}]
ρ_B	Sediment bulk density [g cm^{-3}]
υ	Kinematic viscosity [cm^2 s]

Hydraulic Variables

ADV	Acoustic Doppler Velocimeter
H	Stream depth [m]
HRT	Hydraulic Residence Time
Re_*	Local shear Reynolds number [dimensionless]
u_*	Shear velocity [m s^{-1}]
u, v, w	Streamwise, transversal and vertical velocity components [m s^{-1}]
u', v', w'	Streamwise, transversal and vertical fluctuating velocity components [m s^{-1}]
τ_{RS}	Local bed shear stress [g cm^{-1} s^{-2}]

Miscellaneous

C_T	Cycle threshold
DEA	Denitrification Enzyme Activity
E	qPCR Efficiency [%]
LINX	Lotic Intersite Nitrogen eXperiment

PCR	Polymerase Chain Reaction
qPCR	Quantitative Polymerase Chain Reaction
R^2	Coefficient of determination
Redox	Reduction/oxidation

1 Introduction

1.1 Background

Since 1970, global reactive nitrogen (N) creation has increased by 120% (Galloway et al. 2008). Through direct production and indirect mechanisms, humans are currently creating more than 400 billion pounds of reactive N per year. This is more than double the amount of reactive N created naturally by biological N fixation, lightning strikes, and volcanic eruptions (Townsend & Howarth 2010). This increase is due partly to expanding industrial emissions from fossil fuel combustion, but mostly to reactive N production via the Haber-Bosch process. These N compounds are the primary nutrients in fertilizer applied to agricultural fields and account for approximately two-thirds of anthropogenically created N (Townsend & Howarth 2010). For common crops such as wheat, corn and rice, N use efficiency of applied fertilizer is often less than 40%, meaning more than half of the fertilizer applied to agricultural fields with these crops is not used for plant biomass (Canfield et al. 2010). When this N is unused by the crop or soil microorganisms it can be volatilized (N vaporized in the form of ammonia (NH_3)) or lost as surface runoff or groundwater leaching. This N leached into soils or carried as overland runoff inevitably ends up in aquatic ecosystems downstream of its application point and leads to degrading water quality in the form of eutrophication, decreased biodiversity and an increase in severe algal blooms (Cardinale 2011; Lewis et al. 2011). In addition, N that is not retained in upstream watersheds propagates to coastal estuaries and off-shore marine environments creating hypoxic and anoxic conditions (Diaz & Rosenberg 2008; Cai et al. 2011). In some cases this can lead to a complete loss of aquatic life.

Due to these concerns, processes which can remove N from watersheds are of increasing scientific interest. N flux in its varying forms has been studied in great detail both *in situ* and in a

laboratory setting and has been modeled at both large (regional) and small (batch) scales. Contingent with our ability to measure N flux is the capacity to locate areas which favor N reduction processes, such as the fluid flow delivery of nitrate (NO_3) and organic carbon (C) to the sediment bed. This thesis will briefly summarize our understanding of N flux in stream systems, primarily through sediment denitrification, and propose a predictive expression based on field and laboratory data to measure NO_3 flux at the sediment-water interface using hydraulic, chemical and morphological conditions of streams.

1.2 N Biogeochemical Reactions in Streams

In aquatic systems, reactive inorganic N can be found in many different valence states, ranging from -3 for the NH_3 and ammonium (NH_4) ions to +5 for the NO_3 ion (Howarth 2009). These many "stops" along the oxidation and reduction pathways allow for several different metabolic reactions including denitrification, nitrification, ammonification (i.e. mineralization), biological uptake through assimilation and fixation (Bernot & Dodds 2005). Other abiotic processes can retain N in the stream system for an intermediate period of time (e.g. sediment adsorption or burial) or permanently (e.g. NH_3 volatilization). Denitrification, which is the step-wise reduction of the soluble N oxides NO_3 and nitrite (NO_2) to gaseous dinitrogen (N_2) (complete) or either gaseous nitric oxide (NO) or nitrous oxide (N_2O) (incomplete), is a common metabolic reaction in aquatic sediments and is paramount to bacterial metabolism and functioning. It is also the only metabolic process which permanently removes N from aquatic systems (Seitzinger et al. 2006). Historically, this process has been viewed as one carried out by heterotrophic, facultative anaerobes using NO_3 (predominantly due to the low NO_2 concentration in the environment) when oxygen is absent (Smith et al. 1978; Seitzinger et al. 2002). In reality, a host of common bacterial denitrifiers are known to reduce NO_3 and NO_2 in the presence of oxygen (Patureau et al. 2000; Otani et al. 2004; Madigan et al. 2009).

Aquatic denitrification is often thought to be controlled by a number of factors, primarily including NO_3 concentration in the water column (Royer et al. 2004; Pina-Ochoa et al. 2006; Mulholland et al. 2008; Solomon et al. 2009; Findlay et al. 2011), organic C content in the sediment (Garcia-Ruiz et al. 1998; Arango & J L Tank 2008), and the vertical dissolved oxygen (DO) distribution from the sediment-water interface through the sediment column (Kemp & Dodds 2002; Pina-Ochoa et al. 2006). Secondary factors controlling denitrification include water flow rate and hydraulic residence time (HRT), temperature, pH and soluble reactive phosphorus (SRP) as well as sediment characteristics and bacterial metabolism (notably aerobic respiration and nitrification; Bukaveckas 2007; Herrman et al. 2008; Mulholland et al. 2009; Graham et al. 2010). Although the importance of the primary factors is well established, the effect imposed by the secondary factors often goes either overlooked or disregarded.

In terms of fluid flow, researchers have broadly noted that a lower discharge acts to increase N uptake through increased contact of the water with the benthos as well as increased HRT (Pind et al. 1997; Seitzinger et al. 2006). Thus, it is generally stated that a slower flow means greater uptake (e.g. greater denitrification rate during summer baseflow as opposed to directly following a rain event with others variables held equal). The effect of the fluid flow on NO_3 uptake is likely not this simple. At a low fluid velocity, NO_3 may quickly be depleted at the sediment-water interface and within the sediment column with little recharge stemming from the small return flow. Conversely, at high velocities, bacterial communities throughout the sediment column can become stressed due to the overabundance of DO and will likely move deeper into the sediments. This will tend to decrease N uptake as NO_3 and organic C are more limiting in deeper sediments. It is likely that an optimal range of flow characteristics leads to a more favorable set of environmental conditions to promote N uptake.

In addition, the effect sediment characteristics play on denitrification also must be examined in greater detail. Benthic sediments are habitat for the vast majority of denitrifying bacteria and are the substrate to which epilithic plants (which will also hold epiphytic denitrifying bacteria) attach. The type of sediment is often controlled by local geology and stream carrying capacity and can frequently be the defining factor in terms of hyporheic exchange and storage found in streams (Lefebvre et al. 2005). Sediment characteristics such as particle size diameter and porosity are well known to play a role in defining reduction/oxidation (redox) conditions and benthic organic matter (BOM) distribution within interstitial spaces. This is often a delicate balance as the large porosity provided in gravel bed streams tends to inhibit denitrification due to the entrainment of DO while slightly higher porosity in silt and clay loams (as compared to well-sorted sandy loams) acts to increase denitrification by providing more interstitial space for denitrifiers and labile C (Solomon et al. 2009). In fact, many studies have corroborated the positive effect fine sediments play in biogeochemical reactions with NO_3 due to increases in porosity and surface area per unit volume for episammic bacterial denitrifiers (Garcia-Ruiz et al. 1998; Inwood et al. 2007; Solomon et al. 2009).

1.3 Modeling Capabilities in Determining NO_3 Uptake at Varying Scales

Models used to track N transport and transformation in aquatic ecosystems vary greatly in scale and function. Basin scale models, for example, are often utilized to determine N retention within the select basin and are integrated across many subsequent watersheds to determine regional N retention. Two of the most well-known basin scale N models, SPAtially Referenced Regressions On Watershed attributes (SPARROW) used by the USGS (Alexander et al. 2000; Preston et al. 2011) and RivR-N (Seitzinger et al. 2002), are statistical models which use observed N flux measurements, spatially referenced N sources and mass-balance relationships to describe longitudinal variabilities and determine primary source location and reach scale uptake.

Meta-analysis performed by Seitzinger and others (2006) found that the amount of terrestrial N denitrified in a watershed decreases as you move downstream. The greatest amount of denitrification occurs in soils, followed subsequently by groundwater, streams/rivers, lakes/reservoirs and estuaries. However, when taking into account areal coverage of each, soil denitrification rates were only one-tenth that of rivers/streams and lakes/reservoirs. Alexander and others (2000; 2007) utilized SPARROW to show that N loss rates were inversely proportional to stream depth, meaning that most N removal occurs in relatively shallow, low-order streams. The ability of these low-order streams to remove N, through their increased contact with the benthos and often more complex hydrologic flow paths, is the reason for the increased attention these often see in nutrient and isotope tracer additions (Peterson et al. 2001; Findlay et al. 2011).

At the reach scale, reactive transport models utilizing the one-dimensional (1-D) advection-dispersion equation are often applied. The nutrient spiraling model (Newbold et al. 1981), which is a simplification of the advection-dispersion equation assuming only advective transport, has been used frequently to describe reach scale uptake length and velocity in isotope tracer experiments. This modeling approach was modified by adding terms to the 1-D advection-dispersion equation which describe the transient storage qualities of the stream. This altered model, termed the One-dimensional Transport with Inflow and Storage (OTIS) model (Runkel 1998), more accurately predicted nutrient uptake rates in streams as it could account for the transient storage zones which actively increase HRT (O'Connor et al. 2010).

Unfortunately, both of these reach scale models fail to capture heterogeneity in fluid and environmental variables in more than one direction as both assume only longitudinal variation in nutrient concentration. 3-D heterogeneity is common in streams due to turbulent flow and complex hydrologic and geomorphic features. This heterogeneity can drive the flux of solutes from the bulk flow to the sediment bed, which can act as a driver for N uptake at the sediment-

water interface (O'Connor & Hondzo 2008). With the use of spatially referenced cross-sectional measurements in hydraulic and environmental variables, along with ever-increasing computing power, it has now become possible to track N movement in streams in three dimensions.

With an understanding of the biogeochemical processes driving N loss at the sediment-water interface, one can measure reach scale N concentration and retention in the longitudinal, as well as transversal and vertical directions, within the stream. Unlike the less complex 1-D spatial models, such as the nutrient spiraling and OTIS models, which assume constant loss of the given nutrient from the water column to the sediment, a turbulent model using well defined topographic and hydraulic data can resolve with greater accuracy select regions more conducive to N uptake. This can be done with a specified predictive model defined at the sediment-water interface. In this study multiple predictive models are proposed which use field-measured variables known to mediate N flux to the sediment bed including streamwise and shear velocity, water column NO_3 concentration, BOM deposition and bed morphometry. Each of these models will be used in future research to predict NO_3 uptake at the sediment-water interface within a turbulent, 3-D Large Eddy Simulation (LES) model which couples morpho- and hydro-dynamic processes (Khosronejad et al. 2012). Lastly, fluid flow uptake measurements are supplemented with sediment analysis to verify that N lost from the water column is permanently removed from the system via denitrification.

1.4 Scope of Thesis

This research seeks better understanding of the processes governing denitrification in low-order streams, specifically the effect that fluid velocity and turbulence plays. 3-D field data were gathered for hydraulic and environmental variables *in situ* and were supplemented with laboratory sediment core analysis to determine N uptake capacity. Sediment denitrification experiments were used to verify N uptake from the water column to the sediment occurred via denitrification.

The first of these experiments used Denitrification Enzyme Activity (DEA) assays to estimate potential denitrification rates through the creation of N_2O as a proxy for N_2 within a sediment slurry. These data were used to determine local N flux and were compared to physical data measured in the vicinity of the core to gauge the mediating variables for N flux from the bulk flow to the sediment bed. These experiments were performed using ambient stream water which either was or was not amended with nutrients to assess limitation. The second set of experiments used microbiological techniques including quantitative Polymerase Chain Reaction (qPCR) to amplify specific DNA fragments encoding for denitrification-specific enzymes. These data were used to not only verify sediment denitrifier abundance but to determine depth distribution within the sediment column. Both of these experiments were designed to improve understanding of factors regulating spatial denitrifier distribution across the stream channel and in the vertical sediment column and to determine under what conditions denitrifying populations were abundant.

Following this, field and experimental data were combined to create 2 functional models for estimating NO_3 flux from the bulk flow to the sediment bed. The first of these models uses data acquired within the Outdoor StreamLab over 3 summers and a wide array of environmental and hydraulic scenarios. A Gaussian-type function was fit to these data and was dependent on fluid flow and channel characteristics within the stream system. The second model was derived following dimensional analysis on data spanning 5 streams of varying watershed and in-stream qualities. This model incorporated not only stream hydraulic data but also environmental and morphological data and was independent of any bias within predictor variables.

2 Measurement of NO_3 Uptake via Denitrification in Streams

2.1 Introduction

Assessing in-stream N cycling often poses problems due to the many complex N pathways and to the difficulty in determining N end products (Groffman et al. 2006). Denitrification, specifically, has been challenging to study *in situ* due to the ubiquitous presence of its end product, N_2, in nature. The use of ^{15}N-NO_3 as an isotope tracer has received much attention as it allows for the measurement of a rare isotope which can be tracked as it moves through different ecological components in aquatic systems. This method has been used frequently for whole-stream assessments, notably the Lotic Intersite Nitrogen eXperiments (LINX), to determine reach scale N transport and transformation (Mulholland et al. 2000). This method, though, requires expensive laboratory processing and has been used by only a limited (but growing) number of researchers nationwide (Groffman et al. 2006; Mulholland et al. 2008).

Sensitive and low cost determination of denitrification activity in aquatic systems can be achieved with the acetylene-block method (Smith et al. 1978). This method uses acetylene, which is known to block the enzyme that converts N_2O to N_2, to measure denitrification in batch experiments. Acetylene produces N_2O as the terminal end product in denitrification, which eases measurements due to the very small background levels of N_2O in ambient air. This method also allows for a very large amount of samples to be processed, which is advantageous because of the patchy nature of stream denitrification and the tendency for disproportionally small areas, often terms 'hot spots,' to dominate denitrification activity (Groffman et al. 2009). Furthermore, since these samples can be run in controlled environments, the effects on denitrification from processes such as DO inhibition or nutrient limitation can be tested in comparative cores. This method has been used to measure denitrification in nearly every landscape, including terrestrial systems, marshes, streams, rivers, lakes, estuaries and marine environments (Groffman et al. 2006).

Another strategy for determining denitrification in sediments comes from the increasing prevalence of microbiological techniques to locate denitrifying organisms. Genomic DNA encoding for denitrifying enzymes can be extracted from sediment and, through the use of qPCR, are amplified to high concentrations allowing for easy detection with fluorescent technologies. Genes known to encode for denitrification include narG, napA, nirK, nirS and nosZ and have been used in varying levels within the literature (Hristova & Six 2006; Correa-Galeote et al. 2012; L. T. Johnson et al. 2012). The genes found most prevalently (both in nature and published literature) are nirK and nirS and have been discovered in dry soils, groundwater and all of the common surficial aquatic environments (Kim et al. 2010). The measurement of these gene fragments has been used to quantify total denitrifier populations and has been compared with denitrification activity as measured with tracer studies and batch reactions (Knapp et al. 2009; Graham et al. 2010; Mosier & Francis 2010).

2.2 Field Methods

2.2.1 Site Descriptions

Measurements were completed over 3 years and in 5 different first- and second-order stream reaches. In the summers of 2010 and 2011 measurements for fluid flow, environmental and sediment variables were taken exclusively in the Outdoor StreamLab (44°58'57"N, 95°15'19"W) at Saint Anthony Falls Laboratory in Minneapolis, Minnesota. This is a field scale experimental facility with a 40 x 20 m riparian basin encased in concrete. Running the length of the basin is a sand-bed stream with 3 meanders of which the average wavelength is 25 m and the sinuosity is 1.3. Inflow to the stream is provided by a headbox with water supplied by the Mississippi River above the Saint Anthony Falls. Prior to reaching the headbox water is filtered through a 1.27 cm screen and transferred through two 46 cm diameter pipes. Discharge can be controlled through these pipes via an inlet valve. The stream features riffle-pool sections with native grasses along

the banks and a basin with a sandy loam soil. Once river-water flows through this system it is collected in a tailbox to release suspended and mobile sediment and finally drains into a spillway, returning to the Mississippi River below the falls.

During the spring of 2012 additional measurements were taken in Purgatory (44°53'43"N, 93°29'36"W), Bluff (44°49'48"N, 93°33'28"W) and Seven Mile Creeks (44°15'39"N, 94°01'33"W) (Figure 2-1). These creeks were chosen above others in central Minnesota based on their average channel size (width and depth), sustained flow and mean velocity. In addition, these creeks were chosen to give contrasting views to the Outdoor StreamLab based on water column and benthic C and N loads.

Seven Mile Creek is located just south of St. Peter, MN in the Middle Minnesota River watershed, and is a heavily agriculturally-impacted stream which finds its origins in a set of springs and drainages ditches about 9.5 km upstream of its confluence with the Minnesota River (Figure 2-1). Greater than 85% of the 95 km^2 comprising the watershed is cultivated, the vast majority of which is fertilized corn and soybean crops (Nangia et al. 2010). As a result, Seven Mile Creek has very high dissolved N and phosphorus concentrations as well as elevated levels of suspended sediment from increased stream bank erosion and farm-field tillage practices. The watershed slope is generally flat until it approaches Seven Mile Creek Park, when the slope and width increase greatly (2.3% on average) and exposed sandstone bluffs line the floodplain. Bed material in Seven Mile Creek varies from silt to gravel-sized particles and has seen great changes to its channel morphometry following projects to limit bank erosion and control grade (Kuehner 2003). Measurements were taken in 4 transects between the Interstate 169 overpass and the confluence with the Minnesota River within Seven Mile Creek Park. This stretch of the creek has more narrow banks (1-2 m) and a silty loam and gravel substrate.

Bluff and Purgatory Creeks, tributaries within the Lower Minnesota River watershed, represented a contrast to Seven Mile Creek as both were more likely to be N-limited based on lower N:P levels. Bluff Creek is a relatively small watershed (17 km^2) in Chanhassen, MN draining a mix of land uses from upland forests and meadows to increasing urbanization and deforestation in the middle and lower reaches. The mean stream slope is approximately 0.5% with incised banks through most of the stream length (MPCA 2012). Soil in the region is glacial till overlaying dense silt-clay layers. Nutrients in this stream are generally low (total phosphorus concentrations between 0.04 and 2 mg L^{-1} and NO_3 concentrations between 0.2 and 0.5 mg-N L^{-1}) and occasional increases in these variables are usually associated with snowmelt or stormwater runoff (Barr 2010). In 2002 Bluff Creek was listed as impaired by the Minnesota Pollution Control Agency and placed on EPA's 303(d) list due to elevated turbidity levels (MPCA 2012). Since then the stream has also been listed as impaired for stream biota based on a poor fish Index of Biotic Integrity (IBI). Measurements in this creek were taken in 4 transects downstream and under the US Highway 212 overpass in Chanhassen, MN (Figure 2-1).

Purgatory Creek, located east of Bluff Creek in Eden Prairie, MN, begins in Lotus and Silver Lakes in the northwest corner of the watershed and runs through a set of parks and conservation wetlands before entering mostly urban land uses. The total watershed area is 83 km^2 (RPBCWD 2011). Due to the prevalence of wetland marshes and a thick vegetative canopy this stream has higher levels of dissolved organic carbon (DOC) than the other streams studied. Similar to Bluff Creek, nutrient concentrations are generally low and spikes can most often be attributed to spring snowmelt and stormwater runoff in the predominantly urbanized lower reaches of the watershed. Measurements for this study were taken in 2 transects downstream of Purgatory Park and just upstream of the intersection with Scenic Heights Drive (Figure 2-1). Downstream of this site represents the urbanized reach of the stream, whereas upstream of this location is generally more undeveloped and protected.

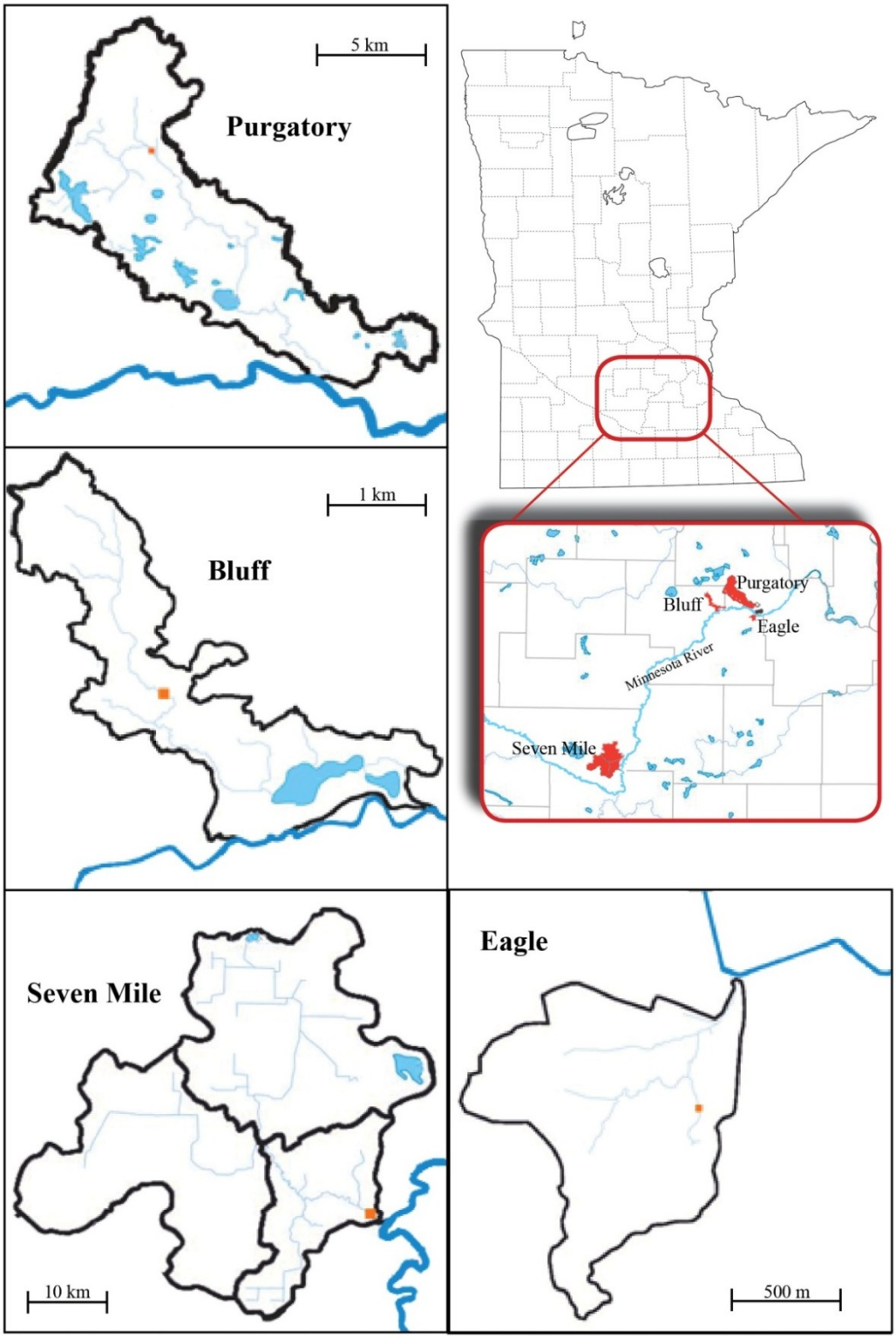

Figure 2-1: Location and delineation of watersheds studied in the late spring and fall of 2012 including (from top left) Purgatory, Bluff, Seven Mile and Eagle Creeks. The orange marker in each watershed signifies the location of measurements.

Lastly, in the summer of 2012, Eagle Creek (44°46'10"N, 93°23'08"W), in Savage, MN, was the site of a nutrient uptake experiment in which sediment cores were extracted to measure denitrification potential. This creek is spring-fed with the only known self-sustaining trout population remaining in the Twin Cities Metropolitan area (MDNR 2012). Eagle Creek's watershed drains into the lower Minnesota River and has a small watershed size of 8.7 km^2, which has been heavily affected by residential and commercial urbanization. Nutrient and DOC concentrations are generally low while the stream is very alkaline (often > 250 mg L^{-1}) and hard (often > 200 mg L^{-1}) due to large groundwater inputs and limited overland runoff (Scott County SWCD 2008). Stream baseflow ranges between 30 and 40 L s^{-1} and is generally constant due to sustained groundwater inputs. Measurements were taken over a 100 m reach in the east branch of Eagle Creek 500 m upstream of its confluence with the western branch (Figure 2-1).

2.2.2 Measuring Equipment

Fluid flow velocity measurements were taken using an Acoustic-Doppler Velocimeter (ADV) (Nortek, San Diego, CA) able to measure in the x (streamwise), y (transverse) and z (vertical) directions. Velocity time-series data were collected at a frequency of 200 Hz for either two or four minutes. Four minute durations were used during initial measurements in the Outdoor StreamLab at high flow with two minute durations used for low flow measurements in the Outdoor StreamLab and in all other streams.

Time-series data were collected for environmental variables across and along the stream including water temperature, DO and NO_3 concentrations. Temperature measurements were taken using the MicroScale Conductivity and Temperature Instrument (MSCTI; Precision Measurement Engineering, Vista, CA). An OX-N DO Microsensor (Unisense, Aarhus, Denmark) was used to measure DO concentration. This is a Clark-type microsensor which utilizes an internal cathode and anode within an electrolyte. NO_3 point measurements were conducted using

the NO_x Biosensor (Unisense) which allows for molecular diffusion of NO_2 and NO_3 ions via an ion-permeable membrane. Denitrifying bacteria located within the biochamber of the unit selectively reduce NO_3 and NO_2 to N_2O, which is detected by a N_20 transducer and converted into an electrical signal. The signal created by the N_20 transducer and the DO microsensor were channeled to separate picoammeters (PA 2000, Unisense) for signal amplification. The analog signal from the temperature, DO, and NO_3 sensors was converted to a digital signal using a Measurement Computing data acquisition 14-bit module (DAQ USB-1408FS, Norton, MA). Measuring frequency for these sensors was 50 Hz throughout experiments. Sampling time at one particular point in the channel ranged from 2-4 minutes, similar to velocity measurements.

A traverse and bracket system was designed to allow for fluid flow and environmental variables to be measured at simultaneous points within the stream cross-section (Figure 2-2). The ADV was mounted to the traverse system to allow movement both along the stream cross-section and in the vertical. A bracket was attached to the shaft of the ADV with 3 pre-drilled holes which were used to affix each of the environmental sensors to the ADV. Placement of these sensors in the bracket system allowed for simultaneous collection of time-series data for all variables.

Due to the availability of the NO_x biosensors, NO_3 measurements in Seven Mile, Bluff and Purgatory Creeks were taken using syringe samples. In this case a Luer-lock style syringe was attached to the ADV clamp system via 1/8" ID flexible tubing, which allowed for sampling at the same location as other environmental variables. NO_3 samples acquired in this fashion were filtered with muffled 0.7 μm Whatman GF/F filters and processed using a cadmium reduction method on a Lachet QC8000 autoanalyzer (Hach Company, Loveland, CO). Grab samples were used to determine background composition of other nutrients. Total dissolved nitrogen (TDN) and DOC concentrations were found using a TOC analyzer (Shimadzu TOC-V CSH, Kyoto, Japan). SRP samples were analyzed following the benchtop protocol of Strickland and Parsons

(1972). NH_3 samples were analyzed using the Lachat autoanalyzer (Hach Company) previously described. In the Outdoor StreamLab and Eagle Creek, other variables such as pH, specific conductivity, and turbidity were monitored using Hydrolab Datasondes (Hach Company) located at the entrance and exit of the stream reaches.

2.3 Laboratory Methods

2.3.1 Sediment Coring and Slicing

Sediment samples were attained following completion of cross-sectional measurements for fluid flow and environmental variables at each site. Replicate and triplicate cores were collected at each cross-section at distinct flow regions (often in proximity to the main flow and near channel banks within recirculation zones). These samples were cored using a transparent, 1' diameter PVC tube 6' in length which was plugged at the bottom directly following extraction to ensure the retention of interstitial water. Cores were acid-washed and rinsed with deionized water prior to use. Three cores were taken at each measuring location with equidistant separation between each core. Two of the cores were used for DEA assays while the third was used for DNA analysis. The cores destined for DEA analysis were transferred to sandwich bags in the field and were immediately put on ice. Cored sediment for DNA analysis was immediately put on ice in the field but frozen at -20°C within 0.5-12 hours depending on the site.

To determine the depth distribution of denitrifier biomass the sediment cores were sliced into distinct regions. To accomplish this a Swingline stationary blade was used with a magnifying incremental guide to ensure accurate slices of the still frozen sediment. Previous analysis of total DNA (all DNA, not just denitrifiers) in sediment samples of the Outdoor StreamLab found an increasing DNA concentration from the sediment surface to approximately 1 cm depth (unpublished data). From 1 cm to 2 cm depth the DNA concentration decreased by an order of magnitude. At 6 cm the concentration had again decreased by an order of magnitude. Previous

Figure 2-2: Photographs illustrating (a) the bracket system, which holds (from left) the NOx-Biosensor, OX-N DO Microsensor, and Microscale Conductivity and Temperature Sensor along with (b) the traverse system, which mounts the ADV and allows for transversal and vertical measurements within the stream and near structures (cross vane shown in this photograph). Stream flow is from left to right in both photographs.

analysis by Inwood and others (2007) corroborated these findings as significantly more denitrification occurred in the 0-2 and 2-5 cm regions than in sediments as far as 1.5 m below the sediment surface (with most in the 0-2 cm region).With this in mind only the top 2 cm of sediment were analyzed for denitrifier biomass. The sediment was cut at the following regions starting at the sediment surface: 0.4 cm, 0.8 cm, 1.2 cm, 1.8 cm and 2.2 cm. The slice representing 0-0.4 cm depth was used to represent surficial sediments. In addition, slices of 0.4-0.8 cm represented sediment at 0.6 cm depth, 0.8-1.2 cm represented 1.0 cm depth, and 1.8 to 2.2 cm represented 2 cm depth. Slices on occasion strayed from these depths by 1-2 mm due to coarseness of the blade and cutting ability. This discrepancy was noted and taken into account when distribution profiles were created. Cores extracted in 2012 in Seven Mile, Bluff and Purgatory Creeks (Eagle Creek was not sampled for denitrifier DNA) were partitioned at 3-5 locations to a depth as high as 6 cm depending on core length and sediment type following similar methodology. The partitioned sediment intended for DNA extraction was immediately transferred to sterile 2 ml Eppendorf tubes and stored at -20°C until analysis.

2.3.2 Denitrification Enzyme Activity Assays

Denitrification rates based on nutrient-amended (DR_A) and unamended (or ambient, DR_U) conditions in sediment samples were measured using DEA techniques, in which acetylene is used to block the complete reduction of N_2O to N_2, leaving N_2O as the terminal end-product during denitrification (Smith et al. 1978; Tiedje et al. 1989). Denitrification rates were then calculated based on N_2O accumulation as a function of sediment bulk density (ratio of dry mass to volume) and incubation time. Sediment samples were removed from the stream using PVC cores, stored at 4°C in sandwich bags and analyzed within 3 days. This was well within the 5 day range found by Findlay and others (2011) to yield no significant decline in denitrifying capacity. Approximately 40 g of sediment (wet mass) were incubated with 40 ml of a DEA amendment solution in “static core” 125 ml Wheaton bottles with rubber septum caps. The amendment

solution consisted of potassium nitrate (100 mg-N L^{-1}), potassium phosphate (14 mg-P L^{-1}), d-glucose (100 mg-C L^{-1}) and chloramphenicol (10 mg L^{-1}) to ensure nutrients were not limiting denitrification rates and that microbial growth (i.e. the synthesis of new denitrifying enzymes) was inhibited (Groffman et al. 2006; McCrackin & Elser 2010). Each bottle was filled to the 40 ml solution volume using ambient stream water to ensure other micronutrients were available to denitrifying bacteria. Oxygen was purged from these bottles using purified helium and 10 ml of CaC_2-generated acetylene was added to each bottle using a 20 cc syringe. These bottles were shaken to homogenize, allowed 15 minutes to settle, and a 5 ml gas sample was extracted via a disposable syringe and used as the initial N_2O concentration. The bottles were then placed on a shaker table and allowed to incubate for 2-4 hours at room temperature (Tiedje (1989) recommends 2-6 hours as NO_3 becomes limiting over a greater time). A final 5 ml sample was extracted and both headspace samples were ejected from the syringe into evacuated glass vials for analysis on a Hewlett Packard (Palo Alto, California) 5890 Series II gas chromatograph equipped with an electron capture detector operating at 300°C. This instrument uses columns (1/8" x 6') packed with the porous-polymer adsorbent Porapak Q (Sigma-Aldrich, St. Louis, Missouri), incubated at 35°C. Helium was used as a carrier gas (30 ml/min) and Argon (95%) and Methane (5%) were combined for the make-up gas. Gas samples were extracted from their vials using a Hewlett Packard 7694 headspace autosampler. Following the second gas sampling, liquid was drained from the Wheaton bottles and the sediment was dried at 105°C. Lastly, the sediment was ashed for 4 hours in a muffle furnace at 550°C to determine the ash-free dry mass (AFDM). N_2O production, calculated from the change in concentration during the incubation time, was corrected for N_2O dissolved in solution using the Bunsen solubility coefficient (Mahne & Tiedje 1995). Denitrification rates were calculated as a function of sediment bulk density (ρ_B) and aerial rates were calculated assuming 6 cm of cored sediment depth, which was the average core depth across all streams.

Amended rates represent the potential for denitrifying enzymes in these streams when nutrients are not limiting. Although different from *in situ* denitrification rates, these rates are comparable across the stream with similar samples (Solomon et al. 2009). To better gauge ambient denitrification rates, samples were taken in the fall of 2012 in Seven Mile, Bluff, Purgatory and Eagle Creeks to compare denitrification rates with (DR_A) and without (DR_U) nutrient amendments. Four cores were sampled in one location and homogenized in a similar fashion to replicate cores. The homogenized sediment was split into 2 sets of replicate batch reactions, each pair used to test either unamended or amended conditions. Amended cores were treated as previously stated with nutrients added to prevent metabolic limitation. Unamended cores contained only stream water and chloramphenicol at a concentration of 10 mg L^{-1} to prohibit the additional synthesis of denitrifying enzymes.

2.3.3 Nir-gene Quantification

DNA was extracted from 500 mg of cored sediment using the Powersoil DNA Isolation Kit (MoBio, Carlsbad, California). The manufacturer's protocol was followed with 5 minute extended durations on the silica membrane to ensure complete elution of DNA through the filter. Following extraction DNA was stored in 10 mM Tris buffer at -20°C. The concentration of DNA in each sample was fluorometrically quantified using the Qubit dsDNA High Sensitivity Assay Kit on a Qubit 2.0 Fluorometer (Life Technologies, Grand Island, New York). DNA concentrations greater than 3 μg ml^{-1} were diluted to less than 3 μg ml^{-1} to ensure no more than 15 ng of DNA in each reaction tube. This was done to reduce the effects of possible inhibitors at higher DNA concentrations. All samples with less than 15 ng of DNA were analyzed at stock concentration.

Copper-containing (nirK) and cytochrome cd_1 type (nirS) nitrite reductase genes were used to detect denitrification in sediment samples (Wakelin et al. 2011). PCR primers were chosen based

on their general specificity and prevalence in the literature (Töwe et al. 2010; Wakelin et al. 2011; Warneke et al. 2011). The nirK primer pairs were nirK876 and nirK1040 and the nirS primers were nirScd3af and nirSR3cd (Henry et al. 2004; Kandeler et al. 2006, respectively).

Quantitative PCR (qPCR) was performed using an ABI 7000 Prism Sequence Detection System (Life Technologies). Each reaction had a total volume of 25 µl containing 10 µM of each forward and reverse primer, 12.5 µl iTaq SYBR Green PCR Supermix (Bio-Rad Laboratories, Hercules, California), 5 µl template corresponding to no more than 15 ng DNA, and Ambien nuclease-free water (Life Technologies) to fill to 25 µl volume. The SYBR Green Supermix contains deoxyribonucloside triphosphates, hot-start iTaq DNA polymerase, 6 mM $MgCl_2$, stabilizers, SYBR Green I dye and ROX internal reference dye.

Thermal qPCR conditions were derived from Henry et al. (2004) with 120 seconds at 50°C followed by 900 seconds at 95°C to activate hot-start polymerases. Subsequently, touchdown cycling was performed beginning with 15 seconds at 95°C to denature the DNA, 30 seconds at 63°C to anneal, 30 seconds at 72°C to extend and 30 seconds for data acquisition by the thermocycler. During the annealing stage the temperature was decreased by 1°C until reaching 58°C. The cycle was repeated 40 more times with an annealing temperature of 58°C. Lastly, a cycle at 95°C for 15 seconds, 60°C for 20 seconds and 95°C for 15 seconds was performed to create a specific dissociation curve.

NirS concentration in sediment samples was determined through the creation of a standard curve using 10-fold dilutions of control DNA ranging in 8 orders of magnitude from 10^1 to 10^8. The cycles at which each of these dilutions fluoresced above a statistical baseline value determined its cycle threshold (C_T). Knowing the established amount of target DNA in each standard and the cycles at which the standard fluoresced yielded the standard curve required to estimate the amount of nir-gene copies in each sample.

Amplification of the nirK product was difficult as the general lack of primer specificity led to gene fragments of varying lengths in the PCR product. Optimization of PCR conditions through changes in reagent and template volume and/or the annealing and melting stage settings was unable to exclude the unwanted gene fragments. Two separate and specialized primer pairs were redesigned following use of the previous primers to increase specificity. The primer length was increased from 17 base pair (bp) on the original primers to 19 and 20 bp on the new ones, respectively. Unfortunately these new primers continued to exhibit similar results. Due to this impediment analysis was only carried out for the nirS gene.

NirS also suffered from non-specific binding but was remedied by running the PCR products on an agarose gel and cutting out the portion of the gel at the desired band length. DNA on the excised gel piece could be extracted using the QIAquick Gel Extraction Kit (QIAGEN, Hilden, Germany) and rerun through similar PCR conditions to further amplify the desired products. This procedure, run for each set of the nirK primer pairs, was still unable to produce only the desired nirK gene fragment without any additional gene lengths.

qPCR efficiency (E) was determined based on the slope of the standard curve as:

$$\mathrm{E}(\%) = \left(10^{\frac{-1}{\mathrm{slope}}} - 1\right) * 100\% \qquad (1)$$

Slopes between-3.92 and -2.92 correspond to efficiencies between 80% and 120%, respectively. 100% efficiency occurs when the PCR product doubles each cycle during the exponential growth phase. If these reactions are more or less efficient than the desired range, product is not created at a rate accurately and precisely measured by the thermocycler. Any experimental run which was more or less efficient than these values (i.e. $E < 80\%$ or $E > 120\%$) was rerun until a more desired efficiency was found. In addition, the variability of each standard triplicate set was analyzed by finding the coefficient of determination (R^2) of the standard curve regression. Any experimental

run with an $R^2 < 0.95$ was rejected and rerun (Hristova & Six 2006). Each sample, along with all standards, was run in triplicate. The average of the triplicates was used as the reported value of gene copies in the sample and normalized by the mass of the sediment in which the DNA was extracted from. Thus each sample had units of gene copies per gram of sediment [g^{-1}].

Lastly, the specificity of PCR performed on nirS gene fragments was confirmed through the sequencing of a clone library. DNA was amplified using conventional PCR in a total volume of 25 µl containing 10 µM each of the forward and reverse primers, 2.5 µl of 10x PCR buffer with 15 mM $MgCl_2$ (Deville Scientific, Metuchen, New Jersey), 2.5 mM concentrations of each deoxyribonucloside triphosphate (Takara Bio, Otsu, Japan), 1.25 U Choice-Taq DNA Polymerase (Denville Scientific), 1 µl of template DNA and Ambien nuclease-free water (Life Technologies) to fill to volume. Conventional PCR was performed using the MJ Research PTC-200 thermocycler (Bio-Rad Laboratories, Hercules, California). Cycling conditions began with an initial denaturation at 95°C for 10 minutes followed by 35 cycles of denaturation at 95°C for 30 seconds, annealing at 58°C for 60 seconds and extension at 72°C for 60 seconds. Lastly, a final extension at 72°C was performed for 10 minutes.

PCR products were separated via electrophoresis on a 2% agarose gel and the desired 410 bp nirS DNA fragment was extracted from a slice of the gel using a QIAquick Extraction Kit (QIAGEN) as previously state. Plasmid DNA was ligated into a vector and cloned into competent DH5α *E. coli* cells using the pGEM-T Vector System (Promega, Madison, Wisconsin). Plasmid extraction was performed using the QIAprep Spin Miniprep Kit (QIAGEN) on isolate clones from each sample. These clones were submitted to the Biomedical Genomics Center at the University of Minnesota and sequenced using the nirS primer pairs previously described. Resulting genomic information was aligned with known nirS sequences within the National Center for

Biotechnology (NCBI) GenBank database using the BLASTN program and homologous nirS sequences were found.

2.4 Data Processing

2.4.1 Velocity Analysis

Velocity data taken in the Outdoor StreamLab were first processed by adjusting the local measuring points to the specialized Outdoor StreamLab coordinate system and then filtered using the modified phase-space threshold method (Parsheh et al. 2010). ADV data acquired in other streams were not rotated but were still filtered using the modified phase-space threshold method. Data collected at each elevation point were processed to find both the mean and fluctuation of each velocity component (u in the streamwise x-direction, v in the transversal y-direction and w in the vertical z-direction). Using the fluctuating velocity components following Reynolds decomposition, the Reynolds stress distribution over stream depth was computed and averaged. Local shear stress at the sediment bed (τ_{RS}) was estimated using two components as:

$$\tau_{XZ} = -\rho_W \overline{u'w'} \tag{2}$$

$$\tau_{YZ} = -\rho_W \overline{v'w'} \tag{3}$$

$$\tau_{RS} = \left[\tau_{XZ}^2 + \tau_{YZ}^2 \right]^{1/2} \tag{4}$$

where ρ_W is the water density and u', v' and w' are the velocity fluctuations in the streamwise, transversal and vertical directions, respectively (Stull 1988). The v'w' expression was often an order of magnitude smaller than the u'w' expression except in the vicinity of the bank (especially at and after the apex of meander bends). Values for Reynolds stresses were extrapolated from the vertical distribution to the bed to evaluate shear velocity (u_*) acting at the bed (Biron et al. 2004):

$$u_* = \left[\frac{\tau_{RS}}{\rho_W} \right]^{1/2} \quad (5)$$

Shear velocities were computed for each vertical velocity profile to determine the local shear velocity acting on the sediment bed.

2.4.2 Statistical Analysis

Statistical analysis was conducted using SAS software version 10.0 (SAS Institute, Inc., Cary, North Carolina). Least-squares regression was utilized to determine trends while parametric datasets were analyzed for significance ($P < 0.05$) using analysis of variance. Non-parametric datasets were analyzed using Mann-Whitney U tests to verify significant differences. Due to a lack of a normal distribution and large range in some of the datasets, data and plots were $\log_{10}$-transformed.

2.5 Results

2.5.1 Environmental Data

Streams draining semi-developed and undeveloped landscapes, including the Outdoor StreamLab, Bluff, Purgatory and Eagle Creeks, generally had low or moderate NO_3 and TDN concentrations (Table 2-1). Conversely, Seven Mile Creek, draining a predominantly agricultural landscape, had NO_3 concentrations greater than an order of magnitude higher than any other stream and TDN concentrations nearly an order of magnitude larger than other streams. NH_3 concentrations were also highest in Seven Mile Creek, but to a much lesser extent, likely due to its preferential and rapid rates of nitrification and assimilation in aquatic systems (Peterson et al. 2001). Stream water temperatures were greatest in the Outdoor StreamLab as measurements were taken in midsummer, whereas measurements in Seven Mile, Bluff and Purgatory Creeks were taken in spring. Measurements in Eagle Creek were taken during midsummer but were lower than other

Table 2-1: Water quality data gathered for streams in this study. Data from the Outdoor StreamLab were acquired during the summers of 2010 and 2011 while data from other streams were taken during the spring and fall of 2012. Reported values are the average acquired over these periods.

Stream Name	NO_3 (mg-N L^{-1})	NH_3 (mg-N L^{-1})	TDN (mg L^{-1})	DOC (mg L^{-1})	SRP (µg L^{-1})	Temperature (°C)
Outdoor StreamLab	0.74	0.11	1.60	11.7	43.3	25.9
Seven Mile	13.22	0.27	15.84	3.2	228.0	15.0
Bluff	0.18	0.03	1.37	9.1	118.5	19.0
Purgatory	0.20	0.13	3.27	13.8	390.0	18.6
Eagle	1.09	0.02	1.29	3.6	7.1	14.4

streams due to groundwater being the main baseflow source for the watershed (Scott County SWCD 2008).

Hydraulic stream conditions were very similar for the Outdoor StreamLab, Purgatory, Seven Mile and Bluff Creeks with low baseflow streamwise velocities of around 0.5 m s^{-1} and average depths less than 40 cm (Table 2-2). Sediment characteristics vary across streams with very sandy, well-sorted sediments in the Outdoor StreamLab and Seven Mile Creek and corresponding mean ρ_B greater than 1.30 g cm^{-3}. Purgatory, Bluff and Eagle Creek sediments contained an increasing amount of silts and clays and therefore ρ_B was generally less than 1.30 g cm^{-3} and oftentimes approaching 1.10 g cm^{-3}. The lower ρ_B values in Purgatory and Bluff Creeks could also be attributed to increases in BOM, as the asymmetrical shape of benthic C can act to increase pore space volume and subsequently decrease ρ_B measurements.

Table 2-2: Hydraulic and morphologic variables across streams.

Stream Name	BOM ($g\ cm^{-2}$)	ρ_B ($g\ cm^{-3}$)	u ($m\ s^{-1}$)	u_* ($m\ s^{-1}$)	H (m)	nirS (g^{-1})	DR_A (mg-N $m^{-2}\ hr^{-1}$)
Outdoor StreamLab	0.05	1.34	0.45	0.053	0.37	4.19×10^4	0.11
Seven Mile	0.13	1.35	0.53	0.053	0.21	3.97×10^3	0.25
Bluff	0.20	1.23	0.48	0.045	0.20	4.18×10^4	1.99
Purgatory	0.61	1.29	0.48	0.050	0.19	1.44×10^5	5.24
Eagle	0.08	1.22	0.21	0.023	0.11	-	1.94

2.5.2 Amended and Unamended Denitrification Enzyme Assays

Denitrification rates were determined by N_2O production in DEA batch reactions and varied widely across streams (Figure 2-3). Sediment samples were extracted and measured for denitrification activity during spring, summer and fall baseflows in 5 streams and rates ranged from 0.02 to 10.1 mg-N $m^{-2}\ hr^{-1}$ and are comparable to other studies of undeveloped and agriculturally impacted streams (Duff et al. 2006: 2.1-16.3 mg-N $m^{-2}\ hr^{-1}$; Pina-Ochoa and Alvarez-Cobelas 2006: 4.05 ± 3.53 mg-N $m^{-2}\ hr^{-1}$, Mulholland et al. 2008: 0.05-10.0 mg-N $m^{-2}\ hr^{-1}$). Rates were highest in Purgatory Creek during spring sampling ranging from 2.9 to 10.1 mg-N $m^{-2}\ hr^{-1}$ and were significantly greater than every other stream. Samples taken in Purgatory Creek in fall, along with samples taken in Bluff Creek in spring and fall and Eagle Creek in summer and fall were between 0.4 and 6.8 mg-N $m^{-2}\ hr^{-1}$. Samples taken in the Outdoor StreamLab in summer and in Seven Mile Creek in spring and fall had the smallest rates, ranging from 0.02 to 0.83 mg-N $m^{-2}\ hr^{-1}$. Interestingly, Seven Mile Creek had the highest NO_3 concentrations of all streams measured by an order of magnitude (Table 2-1) but had much lower denitrification rates as compared to all streams but the Outdoor StreamLab. Similarly, the Outdoor StreamLab had greater than twice the NO_3 concentration as Bluff and Purgatory Creeks (Table 2-1) but had significantly lower rates during both spring and fall (Figure 2-3). These discretions can likely be linked to a lack of water-column and benthic organic C available to heterotrophic denitrifiers in

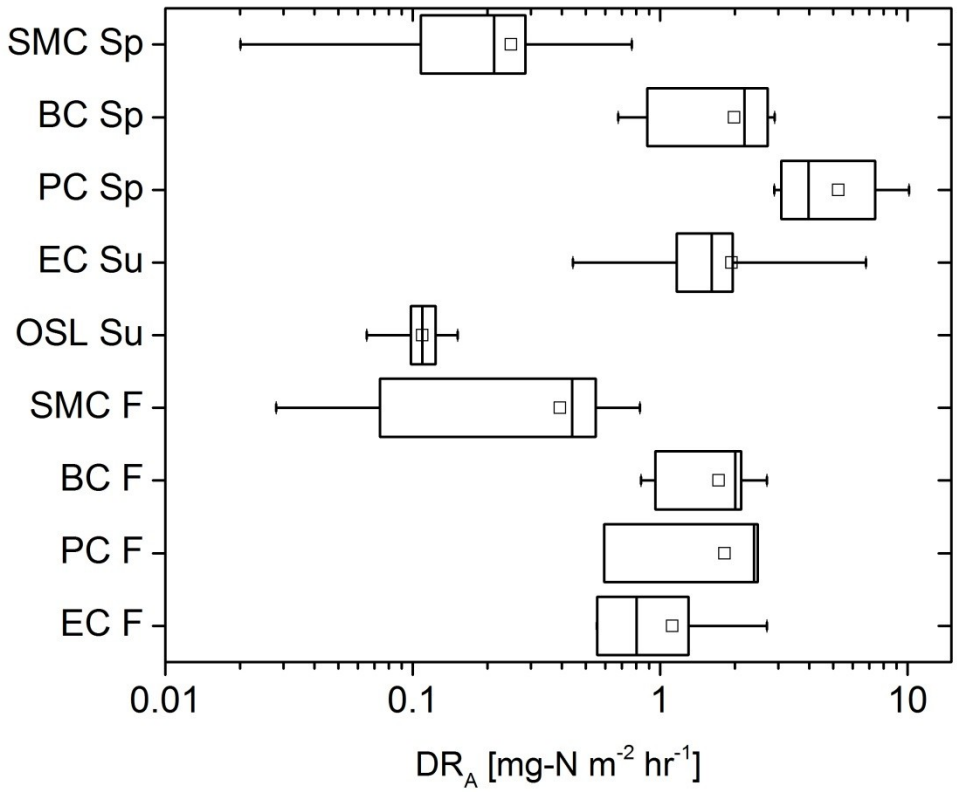

Figure 2-3: Box and whisker diagram illustrating the denitrification rate in nutrient-amended (DR_A) reactions for Eagle Creek (EC), Purgatory Creek (PC), Bluff Creek (BC), Seven Mile Creek (SMC) and the Outdoor StreamLab (OSL) ordered by season: spring (Sp), summer (Su) and fall (F). The length of each box spans the interquartile region (distance between 25th and 75th percentiles). The line through the interior of each box represents the median and the single square inside the box is the mean. The endpoints of each whisker represent the minimum and maximum values recorded. Graph is shown in semi-log scale.

both Seven Mile Creek and the Outdoor StreamLab as compared to the more abundant C concentrations found in the water-column and sediment of Purgatory and Bluff Creeks (Table 2-1, 2-2).

Eagle Creek is a potentially more interesting case in that these measurements were taken during a nutrient tracer injection experiment in which sodium nitrate and sodium chloride were added to the stream. Ambient NO_3 concentration in late summer is often less than 0.1 mg-N L^{-1} but was spiked to better gauge N uptake and reach scale retention in the stream. Although the small amounts of organic C would lead one to assume similar rates of denitrification to Seven Mile Creek and the Outdoor StreamLab, saturated nutrient conditions gave the sediment bacterial community hours to increase its denitrification potential prior to coring.

The effect of amending nutrients to stream water for DEA batch reactions was tested to determine the overall impact in the use of this method and the rate factor increase compared to unamended reactions. Not surprisingly the amendment induced a greater denitrification rate as compared to unamended rates for each stream (Table 2-3, the Outdoor StreamLab was not tested for the effect of amending nutrients). Nutrient amendments had the greatest effect in Bluff Creek, which also had the smallest ambient NO_3 concentration (Table 2-1). Similarly, the effect was also large in Purgatory and Eagle Creeks where NO_3 concentrations are often less than 1 mg-N L^{-1}. In Seven Mile Creek the effect was quite small, with an average doubling of the denitrification rate following amendment, as ambient NO_3 concentrations are very high. Due to the low DOC and BOM concentrations (Table 2-2) in Seven Mile Creek the amendment of C, rather than NO_3, likely lead to the increase in amended denitrification rates during DEA reactions.

Table 2-3: Amended (DR_A) and unamended (DR_U) denitrification rates from DEA batch reactions. The amended rate factor is the ratio of these rates and was averaged across the stream to attain an integrated rate factor.

Stream	DR_A (mg-N m^{-2} hr^{-1})	DR_U (mg-N m^{-2} hr^{-1})	Amended rate factor	Average rate factor for stream
Seven Mile	0.07	0.03	2.23	2.18
Seven Mile	0.55	0.18	3.12	
Seven Mile	0.60	0.50	1.20	
Bluff	2.70	0.20	13.55	7.89
Bluff	2.12	0.27	7.85	
Bluff	0.96	0.42	2.27	
Purgatory	2.47	0.25	10.02	4.87
Purgatory	0.59	0.28	2.16	
Purgatory	2.39	0.98	2.44	
Eagle	1.67	0.25	6.58	6.46
Eagle	0.77	0.28	2.71	
Eagle	1.51	0.30	4.97	
Eagle	2.49	0.97	2.57	
Eagle	6.79	0.73	9.34	
Eagle	1.36	0.11	12.56	

2.5.3 Microbial Nir-gene Analysis

DNA analysis using qPCR had slopes ranging from -3.92 to -3.06 (Table 2-4). This corresponds to efficiencies between 80% and 113% and is consistent with efficiencies found in other published results (Hristova & Six 2006; Knapp et al. 2009; Töwe et al. 2010; Correa-Galeote et al. 2012). All coefficients of determination (R^2) were also larger than the minimum value of 0.95. In 5 of the 10 runs, some $\log_{10}$ copies were excluded. In all but one of these runs they were the most and least diluted standards and was most often outside the measuring range of samples in these experiments. In each of these runs at least 5 $\log_{10}$ dilutions were used to create the standard curve.

Table 2-4: Results of qPCR runs for samples in the Outdoor StreamLab, Purgatory, Bluff and Seven Mile Creeks. Log_{10} copies ranged from 0-8 and were excluded if they significantly deviated from the standard curve linearity.

Run	Slope	R^2	Log_{10} copies excluded	Efficiency (%)
1	-3.37	0.992	0,1,2	98.0
2	-3.25	0.981	0,1	103.1
3	-3.06	0.992	-	112.2
4	-3.14	0.982	-	108.2
5	-3.06	0.993	1,4,8	112.2
6	-3.38	0.970	0	97.6
7	-3.35	0.975	0	98.8
8	-3.34	0.974	-	99.3
9	-3.92	0.988	-	80.0
10	-3.54	0.951	-	91.6

Over-efficiency in the case of runs 2-5 signifies that the PCR product is more than doubling with each cycle. The number of copies is determined by the standard curve in each run and, because this falls within the specified range, should not be a problem. This is true conversely for the under-efficiency found in the remaining runs.

Cross-stream variability in nirS was apparent, with a range of $10^{2.3}$ to 10^{6} gene copies when averaging across all depths taken at a specific location (Figure 2-4). The data sets across the 4 streams did not meet the parametric (normality) constraint of analysis of variance, so non-parametric tests were performed to determine significance. Mann-Whitney U tests were performed separately on each of the stream pairs to verify significant differences ($P < 0.05$). Purgatory Creek had a significantly greater abundance of nirS genes compared to all streams but Bluff Creek (Table 2-5, $P = 0.16$). Conversely, Seven Mile Creek had significantly less nirS genes than every other stream. There were no significant differences in nirS abundance between

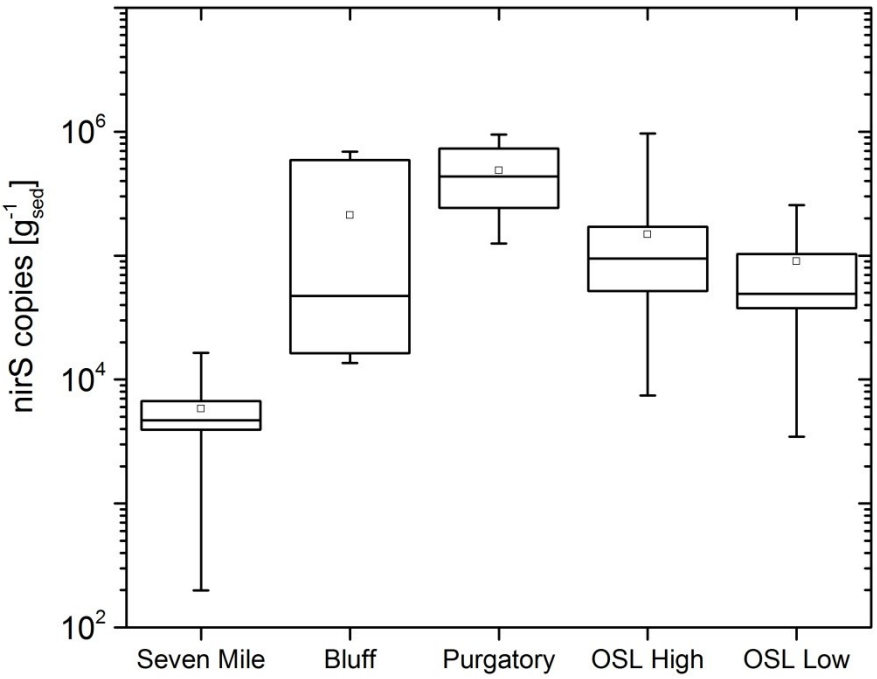

Figure 2-4: Box and whisker diagram illustrating the depth-average range in nirS gene copies for the Outdoor StreamLab (OSL), Bluff, Purgatory and Seven Mile Creeks.

Bluff Creek, the Outdoor StreamLab at high flow or the Outdoor StreamLab at low flow ($P > 0.40$ in each case).

Although not statistically significant, the mean abundance was slightly greater at high flow as compared to low flow in the Outdoor StreamLab (Table 2-5, Figure 2-4). Similarly, the mean in Bluff Creek is slightly higher than both (again, statistically alike) sets of data in the Outdoor StreamLab but has an interquartile range much larger than either data set (Figure 2-4), signifying a large in-stream variability in the abundance of denitrifying bacterial communities.

The samples taken in the Outdoor StreamLab during high flow allow for the most complete analysis due to the larger size of the data set compared to other streams (Table 2-5). The spatial variability of the nirS gene in the Outdoor StreamLab sediment ranges by many factors across the reach and in the vertical column. Numerous samples at varying depths were below the detection limit, signifying either no or very small denitrifying populations. Conversely, the largest sample had approximately $10^{6.58}$ copies. This large range, similar to Bluff Creek, shows the striking heterogeneity that can be found in many streams in not just the bacterial population composition, but also the overall ability of these communities to remove N via their metabolic pathways.

Table 2-5: Depth distribution of nirS copies and total cores extracted for DNA analysis across all streams. Eagle Creek was not included in nirS gene analysis. Samples were extracted from the Outdoor StreamLab (OSL) at both high and low flow scenarios.

Stream Name	Depth-averaged mean (log_{10} copies)	Depth to maximum nirS (cm)	Total cores
Seven Mile	3.8	2.3	9
Bluff	5.3	2.9	7
Purgatory	5.7	2.5	4
OSL High	5.2	1.2	18
OSL Low	5.0	1.3	5

Within each stream denitrifying bacteria were found at all depths but very rarely exhibited a uniform distribution with depth. In the Outdoor StreamLab, denitrifier populations were found in greatest number both near the sediment-water interface and deep within the sediment column. Figure 2-5a shows coring results taken from a transect about 2 m upstream of a rock cross vane placed in the Outdoor StreamLab while Figure 2-5b shows results from a similar transect taken about 4 m downstream of a second cross vane (location in the Outdoor StreamLab shown in Figure 2-6). Both of these cross-sections have abundant denitrifier communities from the sediment surface to 2 cm depth. What differentiates these transects is the location of the largest nirS population. In the upstream portion of the reach they are located near the surface whereas in the downstream portion they are located at a greater depth. In both cross-sections hydraulic properties are similar with shear velocity between 5-7 cm s^{-1} and shear Reynolds values around 20,000. Environmental variables have little time to change over the short (~22 m) traveling distance. The difference between these transects is the location of the measuring points within the reach and, thus, the type and amount of deposition occurring there. Loss on ignition experiments completed following DEA incubations found nearly twice the amount of BOM in the downstream cores as compared to the upstream cores (0.66% compared to 0.34% of sediment dry mass). This is likely due to the lack of imported particulate C following input from the Mississippi River and settling and filtering in the conveyance system between the river and the Outdoor StreamLab as well as the increase in autochthonous C through the Outdoor StreamLab system.

Figure 2-6 gives an aerial view of the Outdoor StreamLab and again illustrates the concentration of the greatest denitrifier populations in the top 0.4 cm of soil in the upstream portion of the reach with denitrifiers at greater and more varying depths in the downstream portion. This pattern is mirrored when comparing the distribution of nirS gene copies to BOM in the stream as the greatest amount of BOM is deposited in the downstream portions of the reach (Figure 2-7).

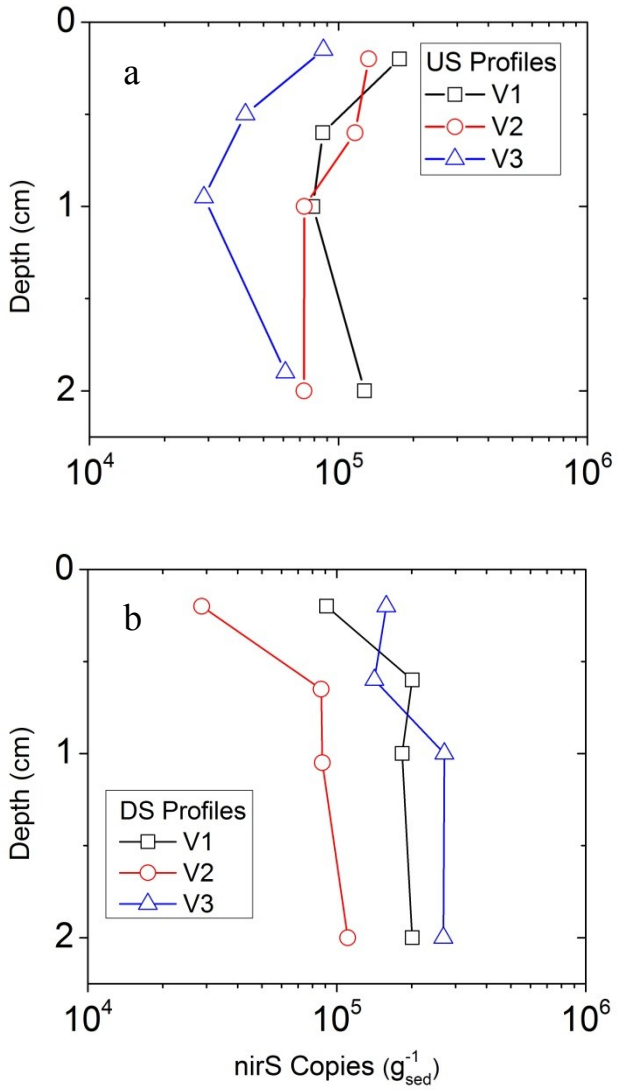

Figure 2-5: Depth distribution of nirS gene copies (a) in the upstream (US) and (b) downstream (DS) portion of the Outdoor StreamLab. V1, V2 and V3 in each graph were separate cores taken along a transect of the stream in varying hydraulic conditions (as noted in Figure 2-6).

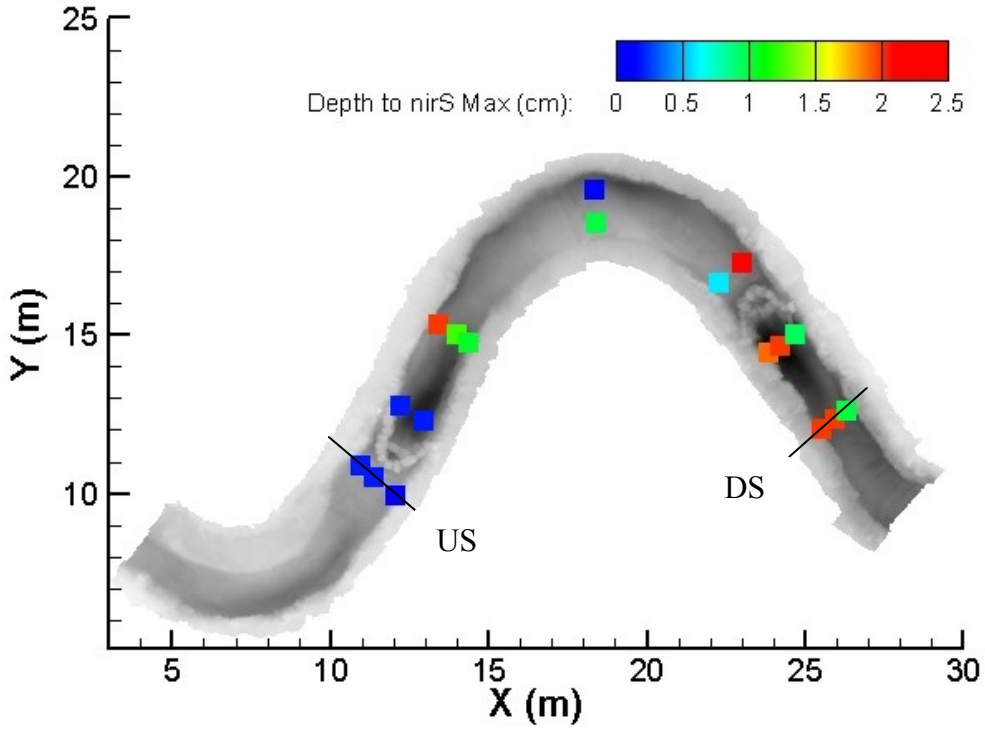

Figure 2-6: Location of cores taken from the Outdoor StreamLab and the depth to the maximum (Max) nirS concentration from each core. Core locations are overlayed on 10 cm resolution topographic data and cross vanes are located at the upstream and downstream portions of the measuring reach. Locations of the upstream (US) and downstream (DS) transects of Figure 2-5 are shown. Flow is from left to right in figure.

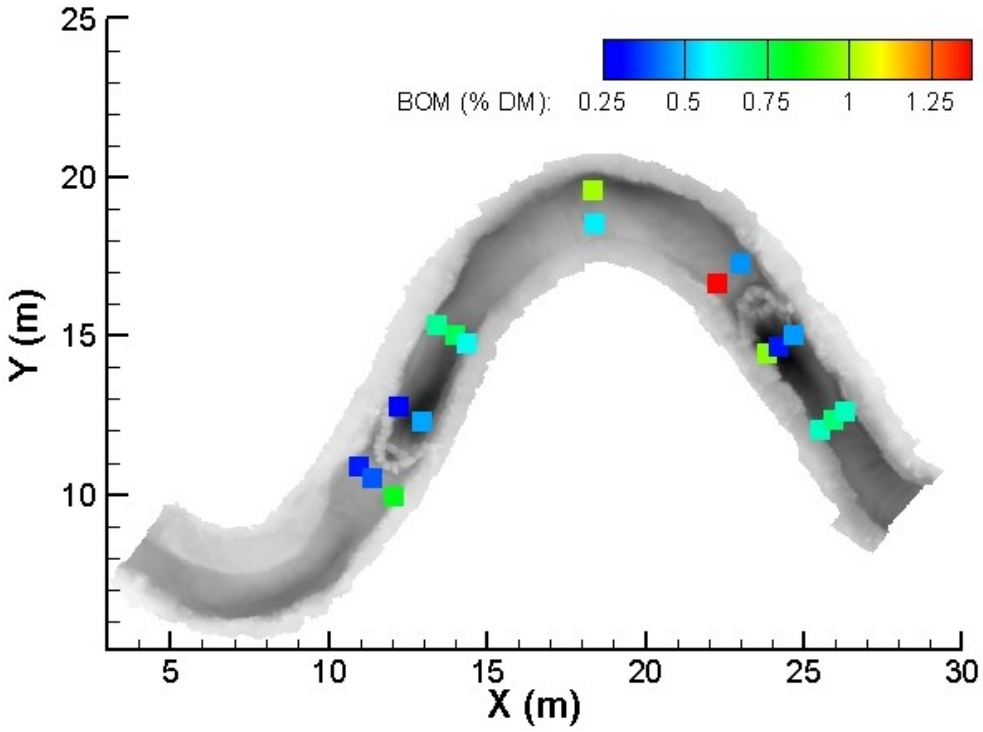

Figure 2-7: Benthic organic matter (BOM), represented as a percentage of sediment dry mass (DM), measured from sediment cores in the Outdoor StreamLab. Flow is from left to right in figure.

The correlation between nirS gene abundance and denitrification potential was measured to determine if nirS was a reliable predictor for in-stream denitrification capacity. For Seven Mile, Bluff and Purgatory Creeks nirS appeared to be a great indicator of potential denitrification rates as determined by DEA batch reactions with a significant correlation between the variables (Figure 2-8a; $R^2 = 0.79$, $P < 0.001$). The relation did not seem to hold for the Outdoor StreamLab, where an increase in nirS gene copies did not foretell an increase in denitrification potential (Figure 2-8b; $P = 0.81$).

2.5.4 Water Quality Cross-sectional and Longitudinal Variability

Cross-sectional measurements of NO_3 concentration, temperature, DO saturation and velocity characteristics were taken to determine spatial variability in factors determining NO_3 uptake in streams. Measurements in the Outdoor StreamLab exhibited this heterogeneity in each variable in all dimensions (Figure 2-9).

N flux to the sediment bed is often determined by NO_3 uptake as NO_2 and NH_3 concentrations are often small and even negligible compared to NO_3 concentration in streams (Table 2-1). NO_3 flux was estimated based on the vertical loss of NO_3 from the water column. Near-bed NO_3 concentration measurements (C_S) were taken between 0-2 cm from the bed and compared to the vertically-averaged NO_3 concentration (C_V) to determine flux either to or from the sediment bed. NO_3 flux was estimated based on this dimensionless concentration (C_V/C_S).

These measurements were performed over 3summers and with varying hydraulic scenarios. As the Outdoor StreamLab has a controlled inlet, discharge could be set for conditions ranging from low flow (25 L s^{-1}) to bankfull (or high) flow (284 L s^{-1}). In addition, rock structure placement was experimentally manipulated to study the influence of hydraulic complexity and turbulence. These conditions are summarized in Table 2-6.

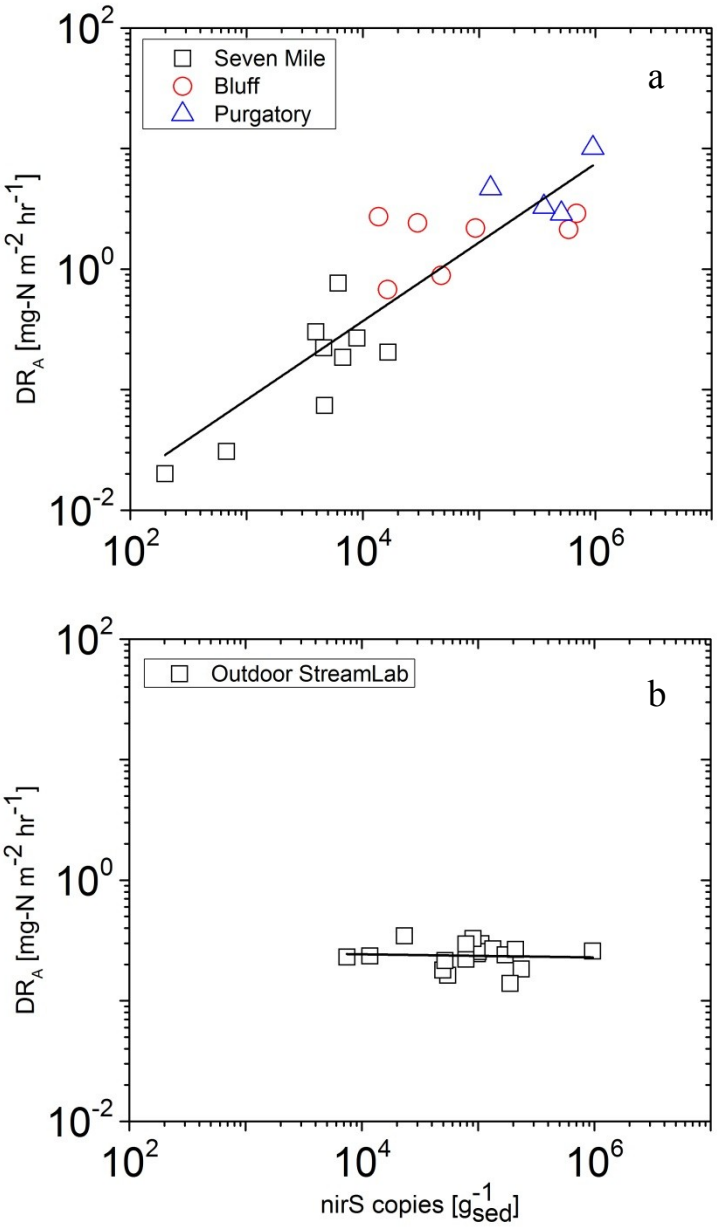

Figure 2-8: Correlation between denitrification potential with amended nutrients and the abundance of nirS copies per gram of sediment mass. There was a strong positive correlation (R^2 = 0.79, $P < 0.001$) for (a) Seven Mile, Bluff and Purgatory Creeks but not for (b) the Outdoor StreamLab ($P = 0.81$).

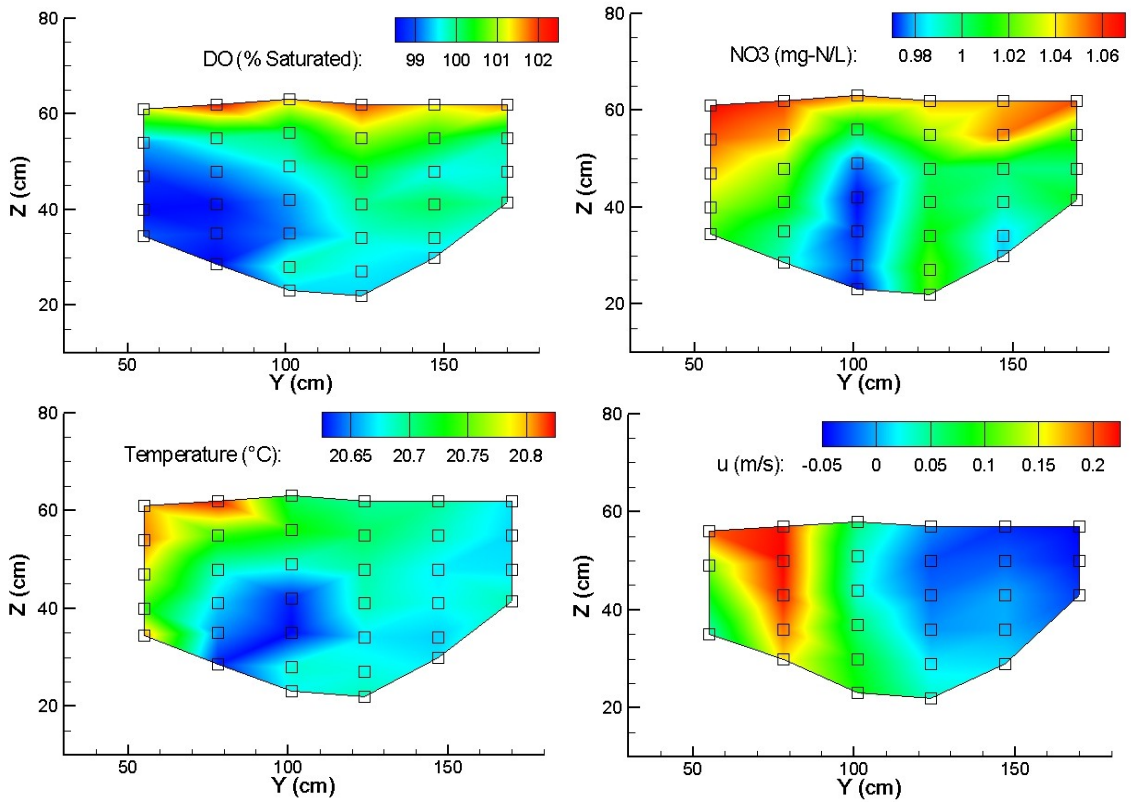

Figure 2-9: 3-D spatial variability in (a) DO, (b) NO_3, (c) temperature and (d) streamwise velocity (u) in the Outdoor StreamLab. These measruements were taken under low flow (Q = 25 lps) conditions during a nutrient tracer injection. Each square in the cross-section represents a data point. View is from downstream looking upstream.

Table 2-6: Hydraulic scenarios run in the Outdoor StreamLab (OSL) in which NO_3 profiles were collected. Values for NO_3 concentration and streamwise velocity (u) are averaged over all cross-sections measured. Bendway weirs were installed in the central meander of the OSL while the cross vanes were installed in previous riffle sections (See Figures 2-1 and 2-6).

Year	Rock structure installed (# in OSL)	Discharge ($L\ s^{-1}$)	NO_3 ($mg\text{-}N\ L^{-1}$)	u ($m\ s^{-1}$)	Transects measured
2009	bendway weir (1)	150	0.74	0.09	1
2010	bendway weir (3)	284	0.46	0.52	3
2011	cross vane (2)	25	1.03	0.10	2

The local shear Reynolds number proved to be a primary indicator for NO_3 uptake over all hydraulic scenarios. Figure 2-10 shows data acquired during time-series measurements which demonstrated vertical uptake of NO_3. Measurements taken near the banks were negated due to additional effects imposed by the boundary. In addition, only points in which C_V/C_S was greater than 1 (i.e. the NO_3 concentration at the sediment is less than the vertically-averaged concentration) are shown in Figure 2-10 as these points denote areas of flux from the water column to the sediment bed and were more likely to be regions of high denitrification. A Gaussian-type function was fit to the data and is of the form

$$\frac{C_V}{C_S} = 1 + 0.68e^{-0.5\left(\frac{Re_* - 17{,}350}{7{,}120}\right)^2} \tag{6}$$

which explained 91% of the variability in C_V/C_S for data points in which $C_V/C_S > 1$.

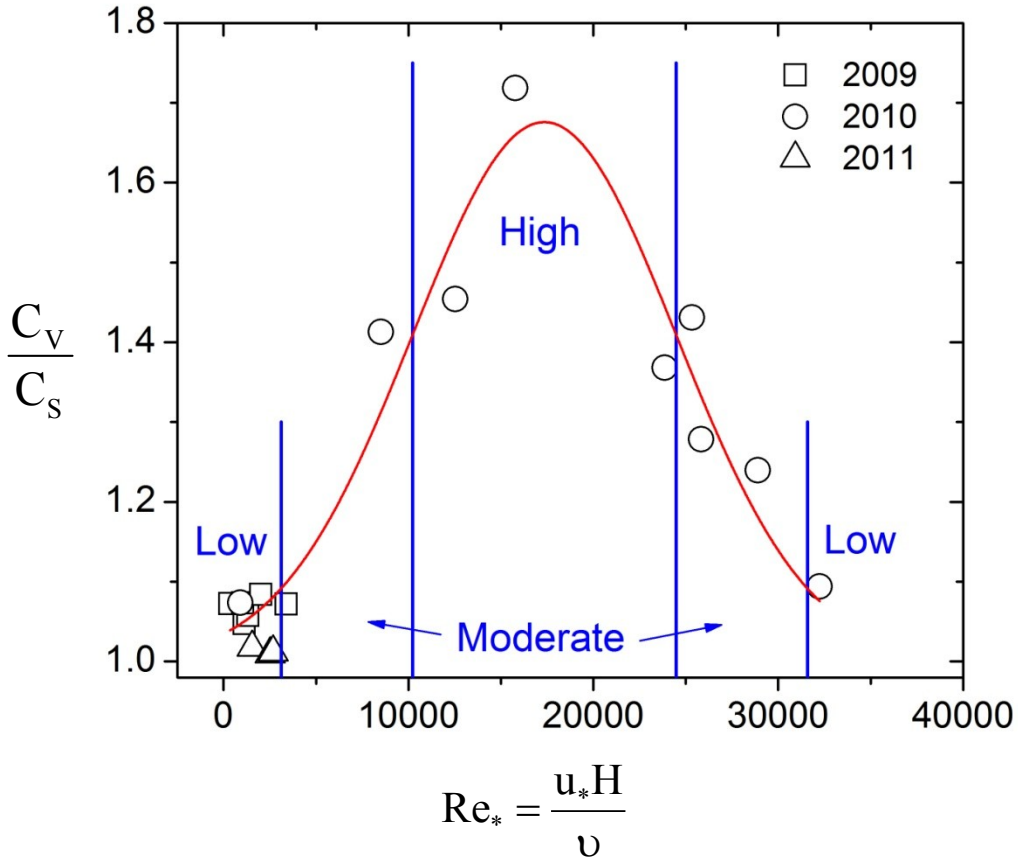

Figure 2-10: Results of time-series experiments showing the relation between the local shear Reynolds number and the dimensionless NO_3 concentration. Areas denoting high, moderate and low NO_3 uptake are labeled.

To determine if C_V/C_S was actually able to estimate NO_3 flux to the sediment bed cores were extracted during bankfull flow sampling in the Outdoor StreamLab in 2011 and analyzed to measure potential denitrification rates. NO_3 flux at the sediment bed in the Outdoor StreamLab is almost completely regulated by bacterial denitrifiers as autotrophs, including filamentous green algae and macrophytes (and therefore heterotrophic epiphytes), occur little in this stream and at the high velocities present when these cores were taken ($Q = 284$ L s^{-1}). Thus it is likely sediment denitrification performed by heterotrophic bacteria is the main pathway in which N is removed (Kemp & Dodds 2002). DEA results found a positive relationship between C_V/C_S and DR_A for cores taken from the Outdoor StreamLab where $C_V/C_S > 1$ (Figure 2-11). This demonstrates that as the sediment bacterial community increases its ability to denitrify it draws down the NO_3 concentration at the sediment-water interface and increases the vertical concentration gradient.

Equation (6) is based on hydraulic conditions in which momentum flux from the stream channel to the sediment bed, depicted by the local shear Reynolds number, is a primary driver for NO_3 uptake from the bulk flow to the sediment-water interface (O'Connor & Hondzo 2008). This predictive model indirectly includes effects from temperature, DO saturation and sediment characteristics but does not explicitly include them in the calculation. In addition, as points in which $C_V/C_S < 1$ were not included in analysis this model is unable to determine areas in which NO_3 flux is from the sediment to the bulk flow (e.g. nitrifying regions).

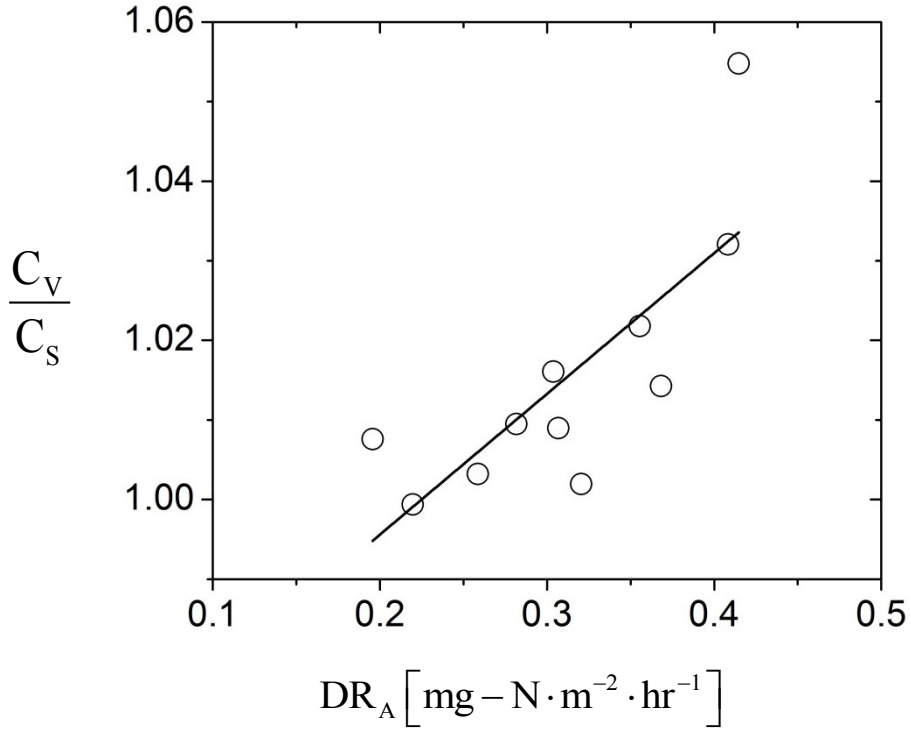

Figure 2-11: DEA results exhibiting a positive relationship between denitrification rates for amended samples (DR_A) and dimensionless NO_3 concentration ($R^2 = 0.56$, $P = 0.005$) found in replicate cores in the Outdoor StreamLab.

3 NO_3 Flux at the Sediment-water Interface as Determined by Dimensional Analysis

3.1 Introduction

The magnitude and direction of NO_3 flux at the sediment-water interface depends on a host of factors, most notably turbulence characteristics, water quality, bed substrate type and geomorphology. As stated in chapter 1, NO_3 uptake via denitrification can be enhanced or inhibited by water quality variables including the concentration of NO_3, DO and labile organic C, temperature, pH and SRP as well as hydraulic variables including fluid flow velocity and HRT, (Kemp & Dodds 2002; Royer et al. 2004; Pina-Ochoa et al. 2006; Arango et al. 2008; Herrman et al. 2008; Findlay et al. 2011). Sediment characteristics including particle size, sorting and bedform height also play a role (Inwood et al. 2007; Solomon et al. 2009). In an idealized scenario, each of these variables would be included in analysis. In reality, a multivariate approach including many, but not all, of the most important variables should provide strong predictive capabilities.

Predictive models for NO_3 flux via denitrification at the sediment-water interface have been derived using a host of methods, including the use of the acetylene-block method, ^{15}N isotope studies and mass-balance calculations. Bohlke and others (2009) compiled data associated with the LINX I study and found a relation involving just NO_3 concentration predicted much of the variability in the dataset. Alexander and others (2009) used the SPARROW model and denitrification rate values compiled from a literature review to create regression-based equations from water discharge, depth, in-stream NO_3 concentration and temperature data. Seitzinger and others (2006) similarly compiled denitrification data from the literature to produce a predictive expression based upon stream hydraulic conditions. Other predictive expressions are summarized

in Table 3-1 and were compiled from aquatic systems around the globe using a host of methods including multivariate (or multiple) regression and dimensional analysis. These expressions vary greatly in both their predictive capabilities as well as the array of variables needed to adequately resolve the contrast in benthic denitrification rates.

Modeling technologies ranging from watershed to reach to sediment scale use a combination of these functions and methods to determine uptake mass. The SPARROW (Alexander et al. 2009) and River-N models (Seitzinger et al. 2006) utilized their respective predictive expressions to determine reach scale uptake and sequentially integrated these values from upstream moving downstream to determine watershed scale retention. This approach, though, assumes homogeneity in all variables at the sub-reach scale and fails to resolve the sub-reach variabilities than can drive biogeochemical reactions in benthic sediments. Denitrification, as well as other biotically-driven reactions, occurs in a very patchy nature within the benthos and modeling at any scales greater than sub-reach can greatly increase model uncertainty. Determining which variables predominantly drive denitrification and resolving these variables at the greatest feasible resolution will clearly allow for the most accurate determination of reach and watershed scale uptake.

To elucidate which variables were mediating NO_3 flux via denitrification, dimensional analysis was utilized. This is a method which combines the physical parameters that describe a problem in such a way as to produce new, nondimensional variables (i.e. “similarity criteria”) that may aide in the simplification of a complex issue. Dimensional analysis becomes most practical when many independent variables are acting individually (and oftentimes collectively) to affect the overall system, as is the case in denitrification. In addition, when scaling between variables

Table 3-1: Predictive models for NO_3 uptake via denitrification from selected datasets and literature reviews.

Reference	Variable(s)	System	Model analysis	R^2	Denitrification rate measurements
Bohlke et al. (2009)	NO_3	Streams/Rivers	Non-linear Regression	N/A	*in situ* sediment $^{15}N_2$ isotopes Reach scale ^{15}N isotopes Sediment core N_2 and $^{15}N_2$ isotopes
Alexander et al. (2009)	Discharge Height NO_3 Temp	Streams/Rivers	Multiple Regression	N/A	Reach scale ^{15}N isotopes Sediment core DEA in situ sediment $^{15}N_2$ isotopes
Seitzinger et al. (2006)	Depth HRT	Rivers and Lakes	Multiple Regression	0.73	Sediment core DEA Mass-balance calculations
Seitzinger et al. (2006)	Depth HRT	Streams/Rivers	Multiple Regression	0.43	
O'Connor et al. (2006)	NO_3 Depth/Width BOM DO Flux Shear Velocity Kinematic Viscosity Roughness Height	Streams/Rivers	Dimensional Analysis	0.6	Sediment core DEA
Garcia-Ruiz et al. (1998)	Sediment $\%H_2O$ NO_3	Streams/Rivers	Multiple Regression	0.64	Sediment core DEA
Watson et al. (1994)	Exchangeable Magnesium Bulk Density	Terrestrial	Step-wise Multiple Regression	0.81	Sediment core DEA

becomes a barrier to registering trends in data, dimensional analysis can be employed to create similar terms which can then be used to better understand the problem.

In this study, environmental and hydraulic data across 5 stream systems draining differing land uses in central Minnesota were compiled to develop dimensionless similarity criteria and to determine local NO_3 flux via denitrification. Buckingham's pi-theorem was used to derive the similarity criteria and dimensional analysis was performed to generate a pair of predictive expressions based on both amended and unamended DEA reactions. Each predictive expression was dimensionalized to remove cross-term bias and explained 75% and 60% of variability across the full dataset for amended and unamended reactions, respectively.

3.2 Methods

Generally with dimensional analysis Buckingham's pi-theorem is used to determine the number of dimensionless groups necessary to define a problem (Buckingham 1914). In this case the challenge was determining the amount of NO_3 that was lost from the water column to the sediment bed through NO_3 reduction to gaseous products, or denitrification. This biogeochemical reaction is primarily performed by benthic denitrifying bacteria and is governed by a host of seven variables at the local level:

$$J_{NO_3} = f\left(C_{NO_3}, H, u_*, \upsilon, BOM, \rho_B\right) \tag{7}$$

where J_{NO_3} is the rate of denitrification of stream sediments based on DEA assays, C_{NO_3} is the vertically-averaged NO_3 concentration in the water column, H is the stream depth, u_* is the shear velocity, υ is the kinematic viscosity, BOM is the benthic organic matter per area of sediment bed and ρ_B is the bulk density of the sediment. According to Buckingham's pi-theorem, 4 nondimensional groups are needed to describe 7 independent variables with 3 primary dimensions (Buckingham 1914). Repeating parameters were chosen based on their significance in mediating

denitrification and the need to have all primary dimensions described; these included C_{NO_3}, H and u_*. Thus the 4 nondimensional groups $\left(\prod_n\right)$ found using Buckingham's pi-theorem are of the form:

$$\prod_1 = \prod_1 \left(J_{NO_3}, C_{NO_3}, H, u_*\right) \tag{8}$$

$$\prod_2 = \prod_2 \left(\upsilon, C_{NO_3}, H, u_*\right) \tag{9}$$

$$\prod_3 = \prod_3 \left(BOM, C_{NO_3}, H, u_*\right) \tag{10}$$

$$\prod_4 = \prod_4 \left(\rho_B, C_{NO_3}, H, u_*\right) \tag{11}$$

with the nonrepeating parameter in each group followed by the 3 repeating parameters on the RHS of each equation. Solving the dimensional matrix for each group yields the following dimensionless expression:

$$\left\langle \frac{J_{NO_3}}{u_* C_{NO_3}} \right\rangle = f\left[\left\langle \frac{u_* H}{\upsilon} \right\rangle^a \left\langle \frac{BOM}{HC_{NO_3}} \right\rangle^b \left\langle \frac{\rho_B}{C_{NO_3}} \right\rangle^c \right] \tag{12}$$

where the 4 dimensionless groupings are denoted by the $\langle\ \rangle$ sign and the exponents a, b and c will be determined based on the slope of independent plots of each grouping. Dimensionless groups in equation (12) from left to right are termed: dimensionless NO_3 flux, shear Reynolds number, dimensionless benthic C and dimensionless interstitial space. The shear Reynolds number is:

$$Re_* = \frac{u_* H}{\upsilon} \tag{13}$$

This derivation is listed in complete detail in the Appendix. BOM was initially calculated as the amount of AFDM per volume of cored sediment. This value was converted to an aerial average

for use in dimensional analysis by normalizing over the 1" diameter coring tube. Thus the value reported is the amount of C available over the given coring tube area through a depth of 6 cm, which was the average depth of sediment removed for DEA analysis. Bulk density (ρ_B) was determined following DEA measurements as the mass of sediment in each incubation chamber divided by the total volume encompassed by the sediment (including pore space).

Dimensional analysis was performed for both amended and unamended DEA data. Unamended samples represented ambient stream conditions but still had chloramphenicol added to ensure additional bacterial growth was inhibited (thus the total number of sediment denitrifying bacteria are the same in the incubation bottles as in the stream at the time of coring). To determine ambient stream NO_3 flux, amended samples were divided by the denitrification "rate factor" which was determined for each stream as stated previously. Primary analysis was done on previously amended DEA data converted to unamended data using the respective denitrification rate factor for each stream (Table 2-3). This conversion was performed as the calculated in-stream NO_3 flux should best represent ambient conditions in which nutrients may be limiting. As the Outdoor StreamLab sediments were only run with amended DEA reactions, the rate factor from Eagle Creek was used to convert rates to unamended values as the streams share similar nutrient conditions (Table 2-1).

Least-squares regression within a 95% confidence region was used to determine correlation between individual and dimensionless variables used for dimensional analysis. Any values outside the 95% confidence region were excluded from the regression to remove the impact of possible outliers in determining statistical correlations. Log_{10}-transformed plots were used to better showcase the relationship between variables covering large ranges.

3.3 Results

Dimensional analysis was utilized as there were only marginal correlations between NO_3 flux and its governing variables across the 5 streams measured (Figure 3-1). Generally speaking J_{NO_3} was positively correlated with BOM and negatively correlated with ρ_B and C_{NO_3} (Figure 3-1c, e, f). The relationship between BOM and J_{NO_3} seems intuitive as increasing C should increase denitrification as this is the primary substrate used by denitrifiers during NO_3 reduction in sediments. Similarly, the inverse relationship between J_{NO_3} and ρ_B is likely due to the decreasing pore space available to denitrifying communities with increasing ρ_B. The inverse relationship between J_{NO_3} and C_{NO_3} is surprising as a host of previous studies have shown the opposite correlation (e.g. Inwood et al. 2007 and Findlay et al. 2011). There was no definable trend between J_{NO_3} and other variables (Figure 3-1a, b, d).

Solving the dimensional matrix using Buckingham's pi-theorem for amended data found the exponents a, b and c in equation (12) to be -1.56, 1.19 and 1.62, respectively, following separate correlations between each individual dimensionless group and dimensionless NO_3 flux (Figure 3-2). The relationship between the fluid flow dimensionless term, Re_*, and dimensionless NO_3 flux is limited (Figure 3-2a) whereas the relationship between the dimensionless terms describing benthic C and interstitial space are much more defined (Figure 3-2b, c). In the case of dimensionless NO_3 flux versus dimensionless interstitial space an interesting grouping pattern emerges between streams of varying N and C concentrations (Figure 3-2c). Streams with low ρ_B and NO_3 concentration (Purgatory and Bluff Creeks) had the highest values with NO_3 concentrations less than 0.5 mg-N L^{-1} and sediments corresponding to silty clays. Streams with low to moderate NO_3 concentration and moderate to high ρ_B (Eagle Creek and the Outdoor StreamLab) settled in the middle group while Seven Mile Creek, a stream with high ρ_B and a NO_3 concentration an order of magnitude larger than many of the other streams, settled in the lowest

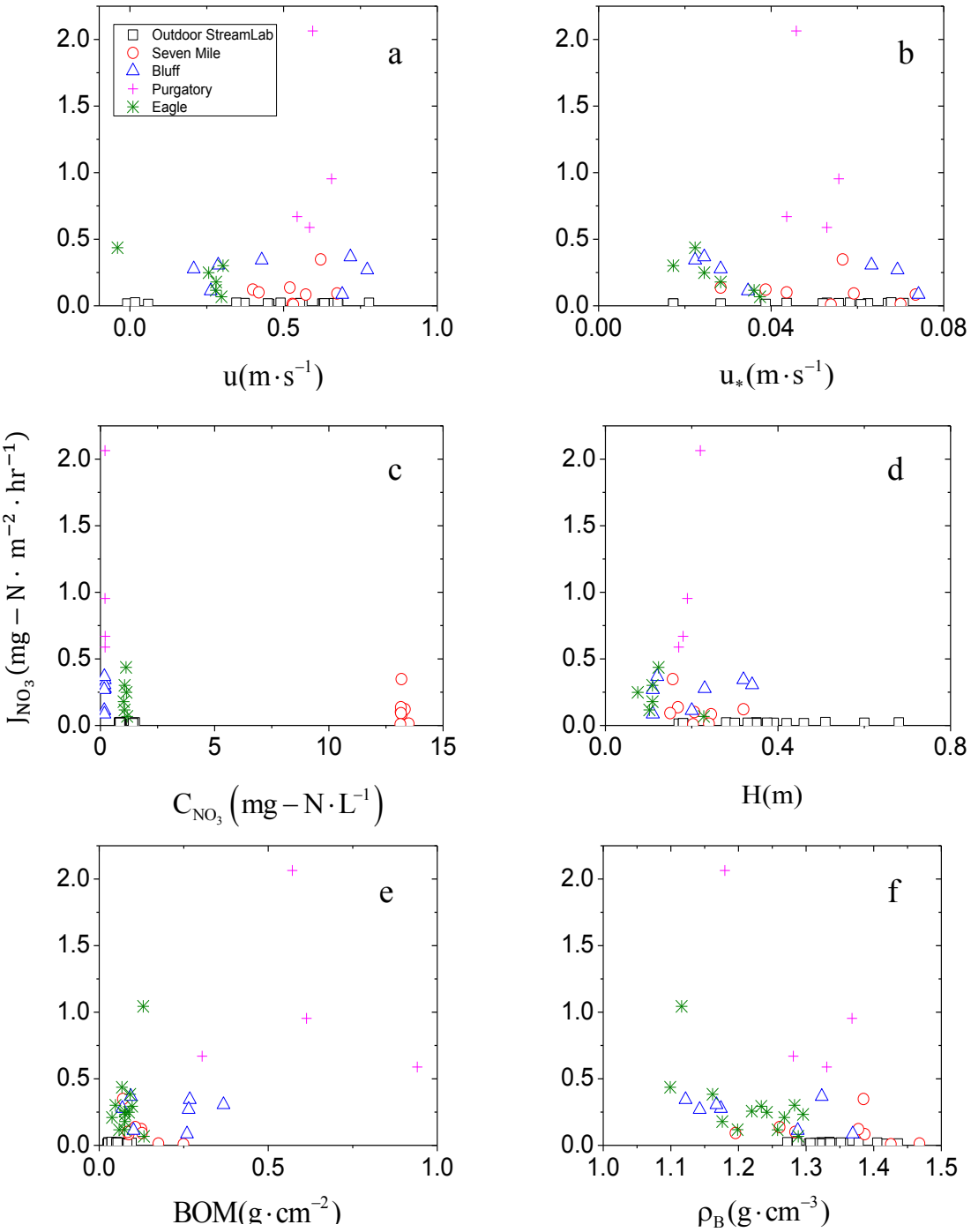

Figure 3-1: Dimensionless NO_3 flux calculated from unamended DEA reactions as a function of fluid flow, morphological and environmental variables including (a) streamwise velocity (u), (b) shear velocity (u_*), (c) vertically-averaged NO_3 concentration in the water column (C_{NO_3}), (d) stream depth (H), (e) Benthic organic matter (BOM) and (f) dry bulk density (ρ_B) of the sediment bed. Field data in these graphs were collected in Eagle, Purgatory, Bluff and Seven Mile Creeks in 2012 and the Outdoor StreamLab in 2011.

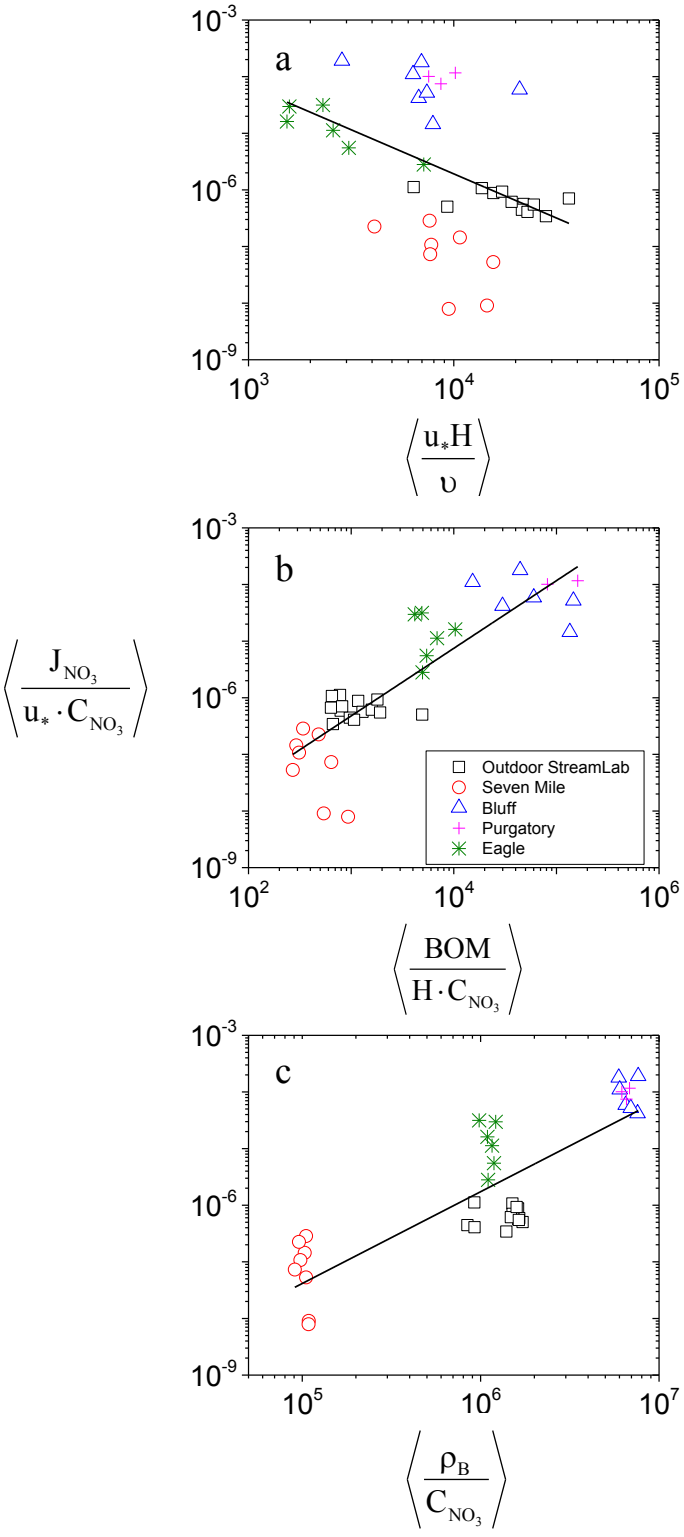

Figure 3-2: Independent plots of dimensionless NO_3 flux using amended DEA reactions against (a) shear Reynolds number ($R^2 = 0.19$, $P = 0.0073$), (b) dimensionless benthic C ($R^2 = 0.74$, $P < 0.0001$) and (c) dimensionless interstitial space ($R^2 = 0.70$, $P < 0.0001$).

group. The dimensionless relation resulting from the utilization of Buckingham's pi-theorem is now:

$$\left\langle \frac{J_{NO_3}}{u_* C_{NO_3}} \right\rangle = 10^{-9.8} \left\langle \frac{u_* H}{\upsilon} \right\rangle^{-5/6} \left\langle \frac{BOM}{HC_{NO_3}} \right\rangle^{5/8} \left\langle \frac{\rho_B}{C_{NO_3}} \right\rangle^{7/8} \tag{14}$$

A log-log plot of this relation (Figure 3-3a) confirms that 88% of the variation in the dimensionless NO_3 flux is explained in the three dimensionless terms on the RHS of equation (14). Due to the prevalence of C_{NO_3} on both sides of the equality and in all but the shear Reynolds term in equation (14) a question arises concerning the possibility for an unnatural correlation (or bias) between dimensionless terms. This possible bias can be removed by dimensionalizing both sides of equation (14) to remove the C_{NO_3} variable form the LHS of equation (14). To accomplish this the slope of the fitted line in Figure 3-3a is used as the exponent of the dimensionless terms in the RHS of equation (14) and the $u_* C_{NO_3}$ term is multiplied on both sides of the equation. Following this J_{NO_3} is plotted against the complete expression which has now been dimensionalized to yield flux units (Figure 3-3b). A fitted regression to this plot in linear scale generates the predictive expression:

$$J_{NO_3}\left[\frac{mg-N}{m^2 s}\right] = 1.8\times10^{-11} u_* C_{NO_3} \left\langle \frac{u_* H}{\upsilon} \right\rangle^{-5/6} \left\langle \frac{BOM}{HC_{NO_3}} \right\rangle^{5/8} \left\langle \frac{\rho_B}{C_{NO_3}} \right\rangle^{7/8} + 4.23\times10^{-5} \tag{15}$$

or in the more common denitrification flux units,

$$J_{NO_3}\left[\frac{mg-N}{m^2 hr}\right] = 6.48\times10^{-8} u_* C_{NO_3} \left\langle \frac{u_* H}{\upsilon} \right\rangle^{-5/6} \left\langle \frac{BOM}{HC_{NO_3}} \right\rangle^{5/8} \left\langle \frac{\rho_B}{C_{NO_3}} \right\rangle^{7/8} + 0.15 \tag{16}$$

This expression still explains much of the variation (75%) found in the dimensionless NO_3 term but now excludes any possible bias created by the preponderance of the NO_3 concentration

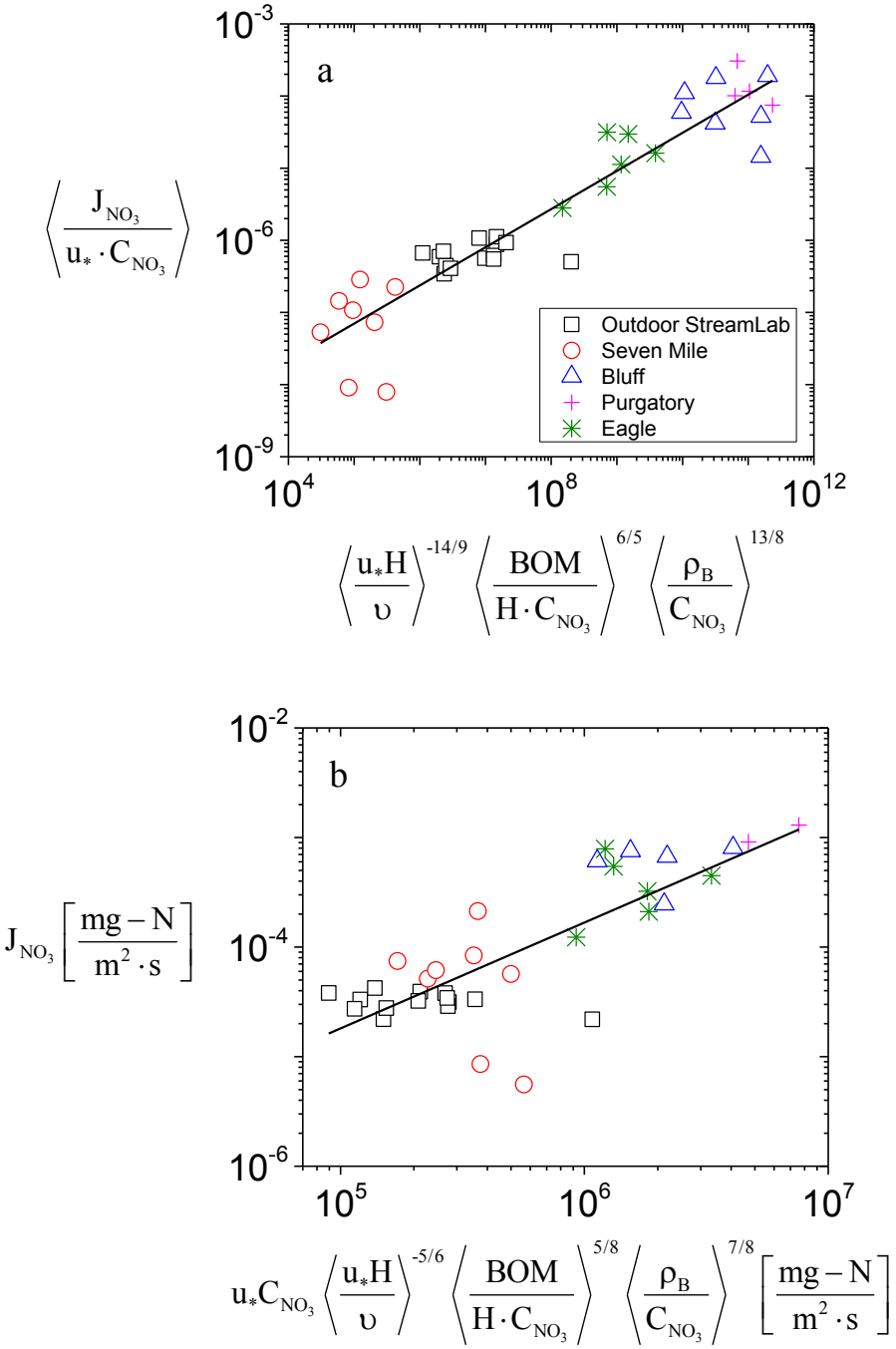

Figure 3-3: (a) Correlation between dimensionless NO_3 flux and other dimensionless groupings ($R^2 = 0.88$, $P < 0.0001$) using amended DEA reactions. The slope of this line ($m = 0.53$) was used to attain the (b) dimensionalized version of equation (14) ($R^2 = 0.75$, $P < 0.0001$). Plot represented in log-log scale to better show trend across the large range in values.

variable in the dimensionless terms on each side of the equality (Figure 3-3b). This relation verifies that NO_3 flux from the bulk flow to the bed is a function of fluid flow characteristics (Re_*, H, C_{NO_3}) as well as stream bed morphometry (BOM, ρ_B) and that the influence of these variables is complex within stream systems.

Dimensional analysis was similarly performed for the unamended data collected in all streams but the Outdoor StreamLab to determine ambient denitrification rates. Independent plots of dimensionless NO_3 flux and each dimensionless term (Figure 3-4) yielded new exponents for equation (12) of -1.54, 1.12 and 1.34 creating the relation:

$$\left\langle \frac{J_{NO_3}}{u_* C_{NO_3}} \right\rangle = 10^{-9.6} \left\langle \frac{u_* H}{\upsilon} \right\rangle^{-9/11} \left\langle \frac{BOM}{HC_{NO_3}} \right\rangle^{3/5} \left\langle \frac{\rho_B}{C_{NO_3}} \right\rangle^{5/7} \tag{17}$$

which explained 85% of the variation in dimensionless NO_3 flux under unamended conditions (Figure 3-5a). Dimensionalizing this equation using the slope of the previous regression yields the predictive function in common flux units:

$$J_{NO_3}\left[\frac{mg-N}{m^2 hr}\right] = 1.23\times10^{-6} u_* C_{NO_3} \left\langle \frac{u_* H}{\upsilon} \right\rangle^{-9/11} \left\langle \frac{BOM}{HC_{NO_3}} \right\rangle^{3/5} \left\langle \frac{\rho_B}{C_{NO_3}} \right\rangle^{5/7} - 0.024 \tag{18}$$

The negative intercept in the above equation can likely be attributed to the limit in the range of data gathered (Figure 3-5b). In the case that the water column NO_3 concentration is zero this function would become undefined as C_{NO_3} is in the denominator of at least one of the dimensionless terms in equation (18). With this in mind the predictive expression should only be used in the range of NO_3 concentrations gathered in this study: 0.16 mg-N L^{-1} < C_{NO_3} < 13.5 mg-N L^{-1}. Similarly, the same can be said for other variables used in dimensional analysis including Re_* (1,000 < Re_* < 50,000), and those listed in Tables 2-1 and 2-2. This predictive model now

allows for both of the major processes mediating NO_3 reduction, the fluid flow delivery of nutrients to the stream bed as well as bed geomorphology, to be described together in one model. The previous predictive model, noted in equation (6), determined NO_3 flux only as a function of the shear Reynolds number and therefore had much lower predictive capabilities.

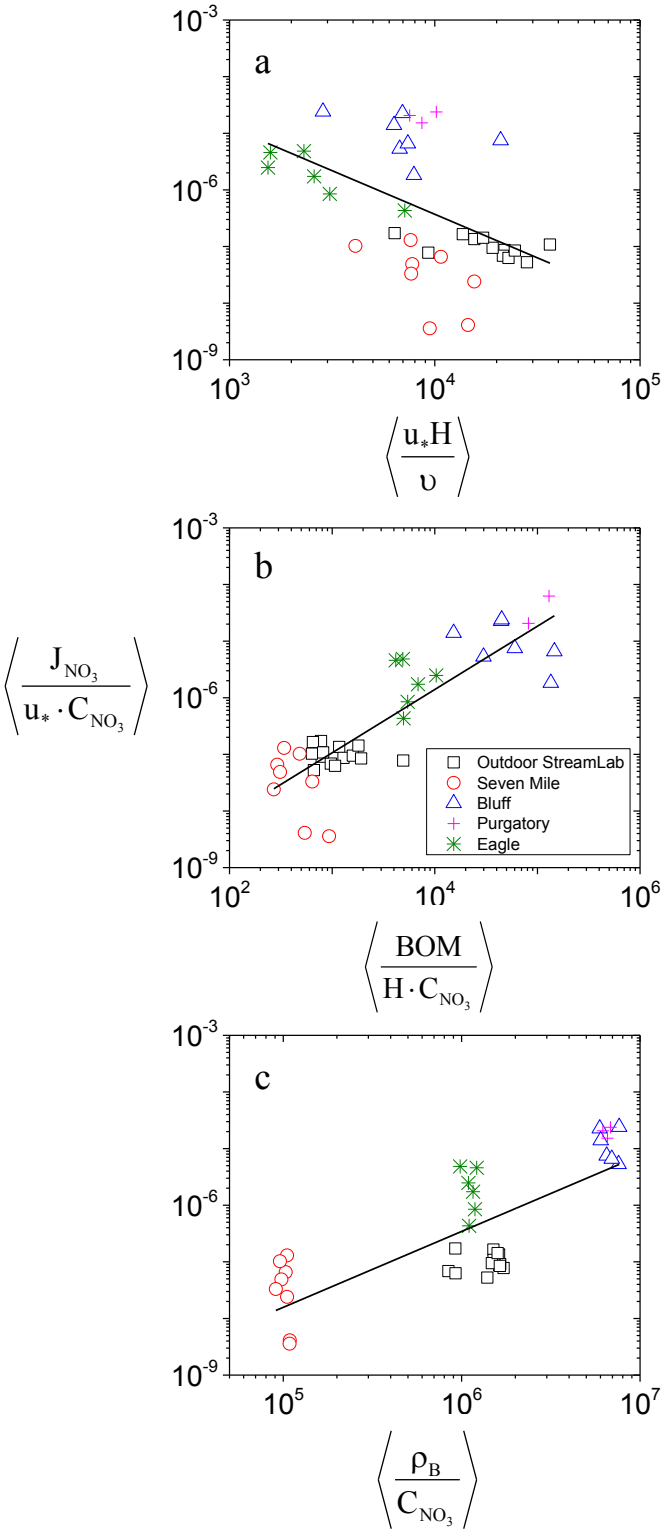

Figure 3-4: Independent plots of dimensionless NO_3 flux using unamended DEA reactions against (a) shear Reynolds number ($R^2 = 0.24$, $P = 0.0027$), (b) dimensionless benthic C ($R^2 = 0.76$, $P < 0.0001$) and (c) dimensionless interstitial space ($R^2 = 0.60$, $P < 0.0001$).

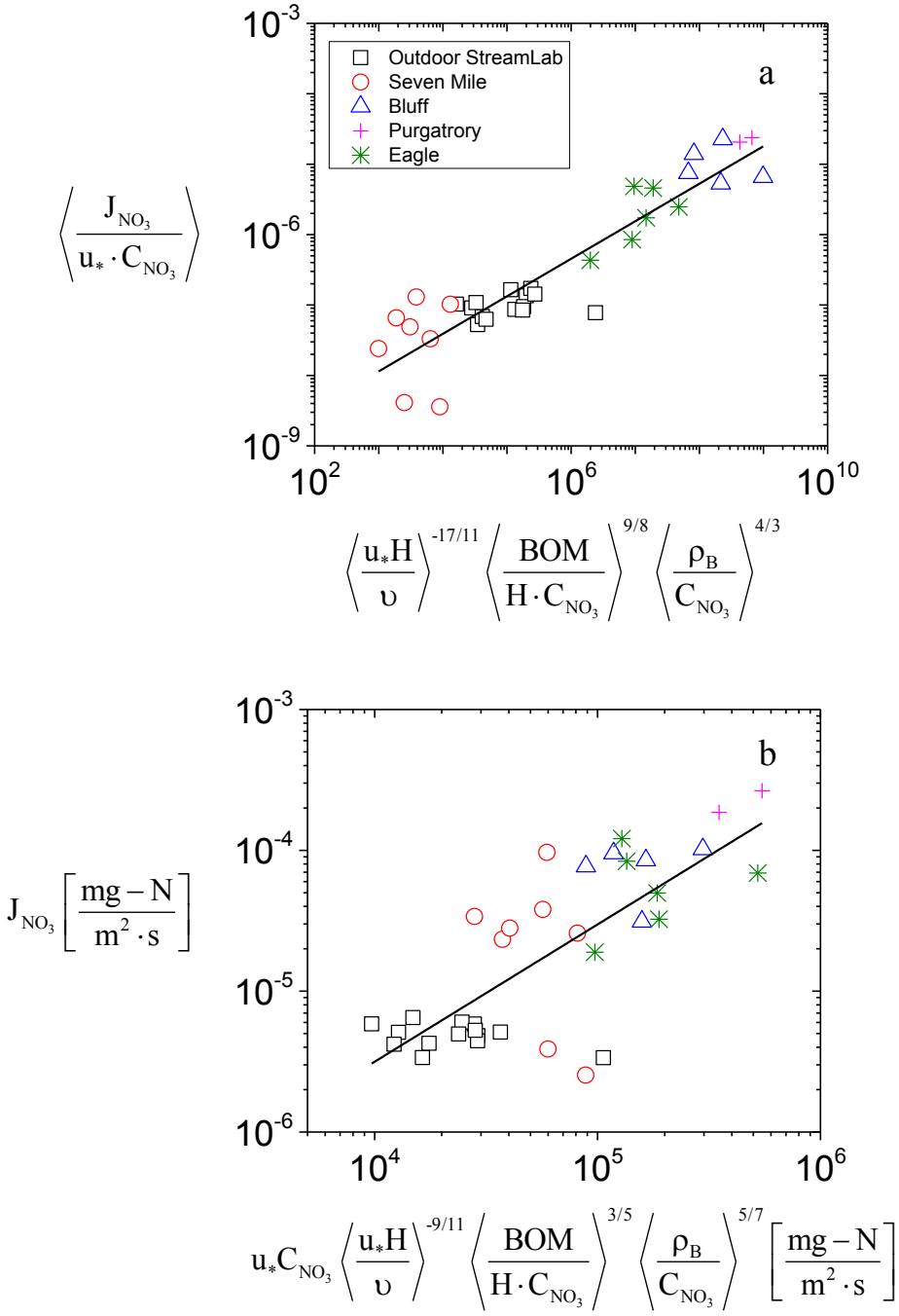

Figure 3-5: (a) Correlation between dimensionless NO_3 flux and other dimensionless groupings ($R^2 = 0.85$, $P<0.0001$) using unamended DEA reactions. The slope of this line ($m = 0.53$) was used to attain the (b) dimensionalized form of equation (17) ($R^2 = 0.60$, $P < 0.0001$). Plot represented in log-log scale to better show trend across the large range in values.

4 Discussion

4.1 Measuring Denitrification in Stream Sediments

Denitrification, measured through the abundance of denitrifying bacteria or with the use of the acetylene-block method, was evident in all streams and at all transects measured in this study. Interestingly, the streams draining semi-developed and undeveloped watersheds exhibited greater denitrification capabilities, with larger denitrifier populations and higher denitrification rates measured in batch reactions. In this way, NO_3 concentration proved to be a poor indicator of denitrification capacity in these streams. This result is contradictory to other studies (Royer et al. 2004, Pina-Ochoa and Alvarez-Cobelas 2006, Mulholland et al. 2008, Solomon et al. 2009, Findlay et al. 2011), and is likely due to the limited availability of C in Seven Mile Creek and the Outdoor StreamLab. The Outdoor StreamLab in particular had high DOC in comparison to the other streams studied (Table 2-1) but had the lowest average BOM (Table 2-2). Low BOM in this stream is likely attributable to the extremely small floodplain size (800 m^2) which increases the impact of DOC supplied by the Mississippi River on in-stream metabolic rates. As large river C is often more recalcitrant due to greater proportions of labile carbon being used in upstream portions of the watershed it is likely the DOC pool did little to increase in-stream metabolism (Thorp & Delong 2002). The semi-developed and undeveloped watersheds of Purgatory and Bluff Creek had greater concentrations of water-column DOC (Table 2-1) and BOM (Table 2-2) which was more likely to be nutrient rich and therefore more conducive to supporting heterotrophic denitrifier populations. It should be noted that these measurements do not paint the full picture of N retention in these streams. NO_3 uptake and denitrification by epilithic biofilms and epiphytic bacteria were not included and could have played a greater role in Seven Mile Creek. Biofilms and macrophytes were sparse within the measuring reach but were much more

evident upstream where tree canopy coverage was reduced. Denitrification in that portion of the reach may be dominated by photoautotrophs and their symbiotic partners.

Bernot and Dodds (2005), based on previous work by Stoddard and others (1994), defined 3 stages for N loading in lotic systems depending on the amount and temporal nature of N import. Stage 1 begins with singular replenishments of N ions due to large runoff events. This leads to Stage 2, in which import and export of N increases due to greater and more lasting events. Lastly, Stage 3 systems suffer from chronically high N concentrations in which singular runoff events are no longer the primary source for input. In this study, Purgatory, Bluff and Eagle Creeks fall into Stage 1 in which runoff events can easily double in-stream NO_3 concentration. The Outdoor StreamLab likely falls into Stage 2, as larger ambient concentrations from the Mississippi River buffer the stream from the impacts of singular storm events. Lastly, Seven Mile Creek can be categorized as a Stage 3 stream with ambient NO_3 concentrations above 10 mg-N L^{-1} due to input from agriculturally-impacted groundwater sources upstream. A review of literature by Bernot and Dodds (2005) noted that N removal rates via denitrification were greatest in Stage 2 streams. In this study it appears Stage 1 streams contained the greatest denitrification capacity (Figure 2-3, 2-4) as the Stage 2 and 3 streams, most notably Seven Mile Creek, may have approached and exceeded N saturation kinetics.

The acetylene-block method has been utilized for determining denitrification rates in streams for more than 3 decades whereas the use of microbiological techniques has only increased in popularity over the last decade (Smith et al. 1978; Throbäck et al. 2004). Studies comparing denitrifier gene abundances to denitrification rates using either the acetylene-block (Mosier and Francis 2010) or ^{15}N isotope tracer (Knapp et al. 2009, Graham et al. 2010) methods have shown varying levels of correlation. Mosier and Francis (2010) found nirS gene abundance to be positively correlated with denitrification rate potentials in estuarine sediments with no correlation

between nirK gene abundance and denitrification rates. Conversely, Graham and others (2010) found nirS and nirK gene abundances to be positively correlated with the coefficient of denitrification (which they stated is a less biased measure of NO_3 loss per unit distance) in stream sediments. O'Connor and others (2006) found a limited correlation between nirK gene abundances and denitrification activity as measured from NO_3 amended batch reactions. This study used nirS gene copies as a predictor for in-stream denitrification potential only, although many studies have linked nirS analysis with nirK and occasionally nosZ (Knapp et al. 2009, Graham et al. 2010, Warneke et al. 2011). For Seven Mile, Bluff and Purgatory Creeks nirS appeared to be a great indicator of potential denitrification rates (Figure 2-8a) whereas there was little predictive capability for nirS in the Outdoor StreamLab (Figure 2-8b). The strong linear relationship for the creeks in Figure 2-8a seems to indicate that nirS is likely the dominating enzyme used by denitrifiers to reduce NO_3, as opposed to nirK or nosZ, and thus gives more confidence in using nirS as the sole predictor for comparing cross-stream denitrification heterogeneity.

The lack of an increase in denitrification potential in the Outdoor StreamLab with increasing nirS gene copies could probably be related to either the exclusion of other prominent genes (including nirK and nosZ) which are regulating denitrification or some error in the DEA batch reactions used to measure denitrification potential. In the case of the samples taken from the Outdoor StreamLab for DEA analysis, there was a small leak in the manifold used to evacuate air from the bottles. This led to a small remainder of ambient air in each sample bottle and oxygen concentrations ranging from < 1% to 18.5% oxygen by percentage of total headspace volume. N_2O production was found in each of the bottles, but it is possible production rates were dampened as some facultatively aerobic denitrifiers continued to metabolize the more electrochemically valuable oxygen ion. Later samples measured in other creeks were properly

purged of oxygen and did show correlation between nirS gene abundance and DEA rates (Figure 2-8a)

Duplicate cores were tested to compare differences between batch reactions amended with nutrients and those which were unamended (only containing ambient stream water with chloramphenicol to inhibit microbial growth). As expected, the amended samples had greater denitrification potential than the unamended samples in every reaction and the ratio of amended to unamended denitrification rates ranged from 1.20-13.55 (Table 2-3). Lower ratios were found in Seven Mile Creek, where high ambient NO_3 concentration helps to enable higher denitrification rates, while greater and more ranging ratios were found in Bluff, Purgatory and Eagle Creeks where either or both of NO_3 and C can limit biological reactions. The high variation across cores taken within each stream can plausibly be attributed to the patchy nature of organic matter deposition. On average, across streams the effect of amending denitrification batch reactions with nutrients acted to increased denitrification rates by a factor of 5.35.

4.2 NO_3 Flux Determination at the Sediment-water Interface

Previous studies have shown the importance in the availability of NO_3 and BOM in providing substrate for bacterial denitrification in sediments (Garcia-Ruiz et al. 1998, Arango and Tank 2008, Mulholland et al. 2008, Solomon et al. 2009, Findlay et al. 2011). Results from this study across 5 stream systems do not support the positive effect of NO_3 in increasing denitrification rates but the overwhelming body of literature speaks otherwise. Conversely, high denitrification rates in Purgatory and Bluff Creeks (Figure 2-3) where DOC and BOM were also high (Table 2-1, 2-2) with low denitrification rates in Seven Mile Creek and the Outdoor StreamLab (Figure 2-3) where DOC and BOM were generally low (Table 2-1, 2-2) illustrate the positive effect of C in increasing denitrification activity in sediments and may be evidence for C limitation in the other streams. C limitation in either Seven Mile Creek or the Outdoor StreamLab may be attributed to

a lack allochthonous input, such as the removal of the dense tree canopy supplying detritus in the case of Seven Mile Creek or the very small basin size in the case of the Outdoor StreamLab, or a lack of autochthonous production, which has often been proven to be the more labile form of C and most likely to be used during bacterial respiration (Thorp & Delong 2002).

Stream and sediment DO concentrations are often considered one of the defining factors (along with NO_3 and C availability) in determining if conditions are conducive to sediment denitrification by facultatively anaerobic bacteria. DO measurements were taken concurrently with many other measurements in this study but the relationship between NO_3 concentration, NO_3 flux and DO saturation was difficult to interpret. Most papers agree that denitrification is prohibited in the presence of DO as bacteria selectively reduce DO instead of NO_3 (Seitzinger et al. 2002; Solomon et al. 2009; Thouin et al. 2009). In reality this biogeochemical reaction is much more complex with anoxic microcosms likely creating habitat in DO saturated sediments or aerobic denitrifiers reducing NO_3 in all benthic environments (Garcia-Ruiz et al. 1998; Patureau et al. 2000). In this study denitrification occurred within streams with near-bed DO concentrations supersaturated (DO > 100%) and in DEA analysis when Wheaton bottles were not properly purged of oxygen (DO ~ 10% gas volume). Although redox conditions in the water column and sediment interstitial space are certainly important in determining which biological reactions will occur within the stream, it was not evident from this analysis what influence bulk flow DO concentration had on sediment denitrification. Without a mechanistic understanding of its effect on NO_3 processing DO was excluded as a variable for dimensional analysis.

Similarly, the effect of pH and SRP in determining denitrification capacity is supplemental to the factors listed in equation (7). Low pH has been shown to inhibit denitrification as electrons are consumed during the reaction, but results are conflicting on the threshold value in which pH begins to have an effect (Baeseman et al. 2006; Herrman et al. 2008). SRP, which is often a co-

limiting nutrient for primary production in lotic ecosystems, has generally had a positive influence on denitrification rates (Graham et al. 2010). This point, though, can be disputed as a greater availability of a co-limiting nutrient may lead to an increase in biotic assimilation and more competition for available NO_3 between denitrifying bacteria and aquatic vegetation. Due to the high uncertainty in the effect of these variables on denitrification they were also excluded from dimensional analysis.

The use of dimensionless terms in simplifying and scaling NO_3 flux dynamics allowed for the generation of a predictive model for NO_3 uptake via denitrification across stream systems. There was a limited correlation between the shear Reynolds number and dimensionless NO_3 flux for both amended and unamended experiments (Figure 3-2a, 3-4a). This either states that fluid flow velocity has a minor role in mediating denitrification in benthic sediments or that the experimental procedure of performing denitrification assays in the laboratory as opposed to *in situ* diminished its effect. By adding chloramphenicol to DEA batch reactions in the laboratory, the community of denitrifiers present at the time of extraction resembles the community during DEA measurements through suppressing the synthesis of denitrification enzymes (McCrackin and Elser 2010). In theory, the community of denitrifiers present at the ambient stream hydraulic conditions will also be present in DEA batch reactions, although they may not denitrify at the same rate. With this in mind nir-gene analysis may be the more appropriate determination for denitrification potential based on hydraulic conditions as the presence of denitrifier DNA is all that's needed to determine denitrification capacity. The dimensionless terms for benthic C and interstitial space exhibited greater correlation with dimensionless NO_3 flux for both amended (Figure 3-2b, 3-2c) and unamended (Figure 3-4b, 3-4c) experiments. Both had a positive relationship with dimensionless NO_3 flux, which is expected as greater amounts of C increases substrate for denitrification and increasing interstitial space leads to more room for denitrifiers between substrate grains.

Unnatural bias between dimensionless variables used to create the predictive model was removed by dimensionalizing equations (14) and (17). Although this reduces the correlation between the predictor and product variables (Figure 3-3, 3-5) it ensures the relationship between the terms is physical, and not just an artifact of the choice in repeated parameters. This cross-term bias was also tested for the dimensionless benthic C and interstitial space terms as increases in C settling can often lead to more uneven sorting of sediments and increasing porosity. Figure 4-1 shows a plot of BOM as a function of ρ_B across all coring locations used for dimensional analysis. No statistical relationship was found between these variables ($R^2 = 0.01$, $P = 0.29$) and verifies there was no bias between these terms which may have artificially augmented dimensionless NO_3 flux.

Stream sites chosen for analysis were all first-order to second-order and exhibited a range in concentrations of NO_3, organic matter and sediment size. Equations (14) and (17) have particular use in the sand-dominated prairie streams of central and southern Minnesota but would be much more limited in the gravel bed rivers of the western United States, for example, as hyporheic exchange processes and redox conditions become much more complex (Bencala & Walters 1983; Hubbard et al. 2010). Arguably the greatest limitation in the dataset is the range of BOM, from 0.02 to 0.95 g cm^{-2}. This is largely due to the timing of these measurements, during late spring and summer baseflows when oftentimes only autochthonous C is available. Similar measurements taken in these streams during early autumn were often greater than 1 g cm^{-2} and as high as 1.4 g cm^{-2} (unpublished data). It is worth noting that equations (14) and (17), similar to equation (6), also suffer from an inability to locate regions with net NO_3 flux from the sediment bed to the water column (e.g. nitrifying regions) or regions where biotic assimilation is occurring. The scope of this research was to spatially resolve denitrification based on varying stream factors and to develop a predictive model to describe inherent variabilities in its distribution. Due to the complexities of including assimilatory N uptake and nitrification into analysis, and as these

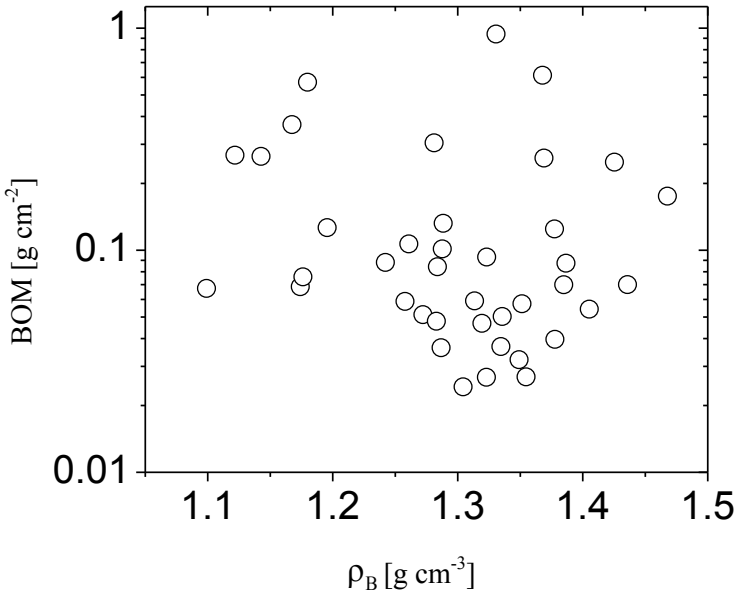

Figure 4-1: Semi-log plot of BOM as a function of ρ_B across streams used in this study. No significant correlation was found between the variables.

processes only result in short-term storage of N in aquatic systems, N flux was only resolved as a function of denitrification. Thus, these predictive models may not be suitable for streams in which biotic assimilation or nitrification is driving N cycling. This would include streams with very low NO_3 concentration or where a thin tree canopy allows for abundant sunlight and dense assemblages of rooted macrophytes (Pinardi et al. 2009). In these environments nitrification may be closely coupled with denitrification in the rhizosphere while biotic assimilation in the water column and sediments is quite high (Forshay & Dodson 2011). Streams with moderate to high NO_3 concentrations and limited sun availability (large tree canopy to reduce photoautotrophic N assimilation) would be preferred as more conducive systems to NO_3 reduction via denitrification (Duff et al. 2006).

5 Research Perspectives and Conclusions

Denitrification is a central process for in-stream N cycling and is paramount to reducing N loading. Although biotic assimilation has been found to dominate N processing in many stream systems, especially during the spring and summer growing periods (Arango et al. 2008, O'Brien et al. 2012), microbially-mediated denitrification remains the most efficient pathway for the permanent removal on N in aquatic ecosystems (Seitzinger et al. 2006). When taking into account indirect denitrification, that is denitrification using previously nitrified or remineralized NO_3, denitrification often accounts for a greater proportion of N processing (Johnson et al. 2012; O'Brien et al. 2012).

As anthropogenically-derived N continues to be problematic for agricultural regions such as the Midwest, determining processes and variables which enhance long-term to permanent reduction in N loads must be studied in greater detail. Increasingly, federal and state governments are reviewing proactive approaches to reducing N import to streams such as nutrient management plans for fertilizer application, cover crops, and riparian buffer strips or denitrifying bioreactors along stream corridors (Schipper et al. 2010). In addition, a greater depth of literature is emerging concerning the efficiency of watershed and stream restoration practices for increasing in-stream N retention (e.g. Lautz & Fanelli 2008; Filoso & Palmer 2011).

Once N reaches the stream, though, it becomes necessary to determine which hydraulic and biogeochemical circumstances enhance NO_3 uptake, in particular by denitrification. This research has found that denitrification is relatively ubiquitous in select stream systems in central Minnesota but can be enhanced or inhibited in the presence of water column and sediment variables including BOM, ρ_B, u_*, H and NO_3. Cross-sectional measurements of fluid flow and environmental variables were paired with sediment coring results to construct predictive models to determine NO_3 uptake by denitrification at the sediment-water interface. With the use of

defined hydraulic and topographical data these expressions can be utilized within a 3-D stream model to determine local NO_3 uptake and provide greater certainty in determining reach scale N retention.

6 References

Alexander, R. et al., 2009. Dynamic modeling of nitrogen losses in river networks unravels the coupled effects of hydrological and biogeochemical processes. *Biogeochemistry*, 93(1-2), pp.91–116. Available at: http://www.springerlink.com/index/10.1007/s10533-008-9274-8 [Accessed October 26, 2012].

Alexander, R.B. et al., 2007. The role of headwater streams in downstream water quality. *Journal of the American Water Resources Association*, 43(1), pp.41–59. Available at: <Go to ISI>://WOS:000244429900005.

Alexander, R.B., Smith, R.A. & Schwarz, G.E., 2000. Effect of stream channel size on the delivery of nitrogen to the Gulf of Mexico. *Nature*, 403, pp.758–761. Available at: <Go to ISI>://000085423100049.

Arango, C.P. et al., 2008. Assimilatory uptake rather than nitrification and denitrification determines nitrogen removal patterns in streams of varying land use. *Limnology and Oceanography*, 53(6), pp.2558–2572.

Arango, C.P. & Tank, J L, 2008. Land use influences the spatiotemporal controls on nitrification and denitrification in headwater streams. *Journal of the North American Benthological Society*, 27, pp.90–107. Available at: <Go to ISI>://WOS:000253203100008.

Baeseman, J.L., Smith, R.L. & Silverstein, J., 2006. Denitrification potential in stream sediments impacted by acid mine drainage: effects of pH, various electron donors, and iron. *Microbial ecology*, 51(2), pp.232–41. Available at: http://www.ncbi.nlm.nih.gov/pubmed/16463131 [Accessed November 28, 2012].

Barr Engineering (Barr), 2010. Bluff Creek TMDL: biological stressor identification. , (March), p.167.

Bencala, K.E. & Walters, R.A., 1983. Simulation of solute transport in a mountain pool-and-riffle stream: a transient storage model. *Water Resources Research*, 19(3), pp.718–724.

Bernot, M.J. & Dodds, W.K., 2005. Nitrogen retention, removal, and saturation in lotic ecosystems. *Ecosystems*, 8(4), pp.442–453.

Biron, P.M. et al., 2004. Comparing different methods of bed shear stress estimates in simple and complex flow fields. *Earth Surface Processes and Landforms*, 29, pp.1403–1415. Available at: <Go to ISI>://WOS:000224604100007.

Buckingham, E., 1914. On physically similar systems: Illustrations of the use of dimensional equations. *Physical Review*, 4, pp.345–376.

Bukaveckas, P.A., 2007. Effects of channel restoration on water velocity, transient storage, and nutrient uptake in a channelized stream. *Environmental Science & Technology*, 41(5), pp.1570–6. Available at: http://www.ncbi.nlm.nih.gov/pubmed/17396643.

Böhlke, J.K. et al., 2009. Multi-scale measurements and modeling of denitrification in streams with varying flow and nitrate concentration in the upper Mississippi River basin, USA. *Biogeochemistry*, 93(1-2), pp.117–141. Available at: http://www.springerlink.com/index/10.1007/s10533-008-9282-8 [Accessed November 5, 2012].

Cai, W.J. et al., 2011. Acidification of subsurface coastal waters enhanced by eutrophication. *Nature Geoscience*, 4(11), pp.766–770. Available at: <Go to ISI>://WOS:000296723500014.

Canfield, D.E., Glazer, A.N. & Falkowski, P.G., 2010. The evolution and future of Earth's nitrogen cycle. *Science*, 330(6001), pp.192–196. Available at: http://www.ncbi.nlm.nih.gov/pubmed/20929768 [Accessed July 13, 2012].

Cardinale, B.J., 2011. Biodiversity improves water quality through niche partitioning. *Nature*, 472(7341), pp.86–9. Available at: http://www.ncbi.nlm.nih.gov/pubmed/21475199 [Accessed July 24, 2012].

Correa-Galeote, D. et al., 2012. Spatial distribution of N-cycling microbial communities showed complex patterns in constructed wetland sediments. *FEMS microbiology ecology*, pp.1–12. Available at: http://www.ncbi.nlm.nih.gov/pubmed/22928965 [Accessed September 18, 2012].

Diaz, R.J. & Rosenberg, R., 2008. Spreading dead zones and consequences for marine ecosystems. *Science*, 321, pp.926–929. Available at: <Go to ISI>://WOS:000258436700028.

Duff, J.H. et al., 2006. Whole-stream response to nitrate loading in three streams draining agricultural landscapes. *Journal of environmental quality*, 37(3), pp.1133–44. Available at: http://www.ncbi.nlm.nih.gov/pubmed/18453433 [Accessed November 29, 2012].

Filoso, S. & Palmer, M.A., 2011. Assessing stream restoration effectiveness at reducing nitrogen export to downstream waters. *Ecological Applications*, 21(6), pp.1989–2006. Available at: http://www.ncbi.nlm.nih.gov/pubmed/21939039.

Findlay, S.E.G. et al., 2011. Cross-stream comparison of substrate-specific denitrification potential. *Biogeochemistry*, 104, pp.381–392. Available at: <Go to ISI>://WOS:000291168900026.

Forshay, K.J. & Dodson, S.I., 2011. Macrophyte presence is an indicator of enhanced denitrification and nitrification in sediments of a temperate restored agricultural stream. *Hydrobiologia*, 668(1), pp.21–34. Available at: http://www.springerlink.com/index/10.1007/s10750-011-0619-2 [Accessed November 28, 2012].

Galloway, J.N. et al., 2008. Transformation of the nitrogen cycle: recent trends, questions, and potential solutions. *Science*, 320(5878), pp.889–892. Available at: http://www.ncbi.nlm.nih.gov/pubmed/18487183 [Accessed July 20, 2012].

Garcia-Ruiz, R., Pattinson, S.N. & Whitton, B.A., 1998. Denitrification in river sediments: relationship between process rate and properties of water and sediment. *Freshwater Biology*, 39, pp.467–476.

Graham, D.W. et al., 2010. Correlations between in situ denitrification activity and nir-gene abundances in pristine and impacted prairie streams. *Environmental Pollution*, 158(10), pp.3225–9. Available at: http://www.pubmedcentral.nih.gov/articlerender.fcgi?artid=3071025&tool=pmcentrez&rendertype=abstract [Accessed November 28, 2012].

Groffman, P.M. et al., 2009. Challenges to incorporating spatially and temporally explicit phenomena (hotspots and hot moments) in denitrification models. *Biogeochemistry*, 93(1-2), pp.49–77. Available at: http://www.springerlink.com/index/10.1007/s10533-008-9277-5 [Accessed October 26, 2012].

Groffman, P.M. et al., 2006. Methods for measuring denitrification: Diverse approaches to a difficult problem. *Ecological Applications*, 16, pp.2091–2122. Available at: <Go to ISI>://WOS:000242849300005.

Henry, S. et al., 2004. Quantification of denitrifying bacteria in soils by nirK gene targeted real-time PCR. *Journal of Microbiological Methods*, 59, pp.327–335. Available at: <Go to ISI>://WOS:000224843300003.

Herrman, K.S., Bouchard, V. & Moore, R.H., 2008. Factors affecting denitrification in agricultural headwater streams in Northeast Ohio, USA. *Hydrobiologia*, 598(1), pp.305–314. Available at: http://www.springerlink.com/index/10.1007/s10750-007-9164-4 [Accessed August 31, 2012].

Howarth, R., 2009. Nitrogen. *The Encyclopedia of Inland Waters*, pp.57–64.

Hristova, K. & Six, J., 2006. *Linking N cycling to microbial community function within soil microenvironments in cover crop systems*, Davis, California.

Hubbard, K.A. et al., 2010. Evaluating nitrate uptake in a Rocky Mountain stream using labelled 15N and ambient nitrate chemistry. *Hydrological Processes*, 24(23), pp.3322–3336. Available at: http://doi.wiley.com/10.1002/hyp.7764 [Accessed November 29, 2012].

Inwood, S.E., Tank, J L & Bernot, M.J., 2007. Factors controlling sediment denitrification in midwestern streams of varying land use. *Microbial ecology*, 53(2), pp.247–58. Available at: http://www.ncbi.nlm.nih.gov/pubmed/17265003 [Accessed November 28, 2012].

Johnson, L.T. et al., 2012. Manipulation of the dissolved organic carbon pool in an agricultural stream: responses in microbial community structure, denitrification, and assimilatory nitrogen uptake. *Ecosystems*, 15(6), pp.1027–1038. Available at: http://www.springerlink.com/index/10.1007/s10021-012-9563-x [Accessed November 2, 2012].

Kandeler, E. et al., 2006. Abundance of narG, nirS, nirK, and nosZ genes of denitrifying bacteria during primary successions of a glacier foreland. *Applied and Environmental Microbiology*,

72(9), pp.5957–5962. Available at: <Go to ISI>://WOS:000240474000035 [Accessed November 12, 2012].

Kemp, M.J. & Dodds, W.K., 2002. The influence of ammonium, nitrate, and dissolved oxygen concentrations on uptake, nitrification, and denitrification rates associated with prairie stream substrata. *Limnology and Oceanography*, 47, pp.1380–1393. Available at: <Go to ISI>://WOS:000178081800010.

Khosronejad, A., Kang, S. & Sotiropoulos, F., 2012. Experimental and computational investigation of local scour around bridge piers. *Advances in Water Resources*, 37, pp.73–85. Available at: http://linkinghub.elsevier.com/retrieve/pii/S0309170811001801 [Accessed November 14, 2012].

Kim, O. et al., 2010. Distribution of denitrifying bacterial communities in the stratified water column and sediment–water interface in two freshwater lakes and the Baltic Sea. *Aquatic Ecology*, 45(1), pp.99–112. Available at: http://www.springerlink.com/index/10.1007/s10452-010-9335-7 [Accessed November 29, 2012].

Knapp, C.W. et al., 2009. Spatial heterogeneity of denitrification genes in a highly homogenous urban stream. *Environmental science & technology*, 43(12), pp.4273–9. Available at: http://www.ncbi.nlm.nih.gov/pubmed/19603634.

Kuehner, K., 2003. Implementation phase of watershed project begnis. *Seven Mile Sentinel*, p.8.

Lautz, L. K. & Fanelli, R.M., 2008. Seasonal biogeochemical hotspots in the streambed around restoration structures. *Biogeochemistry*, 91(1), pp.85–104. Available at: http://www.springerlink.com/index/10.1007/s10533-008-9235-2 [Accessed November 20, 2012].

Lefebvre, S. et al., 2005. Nutrient dynamics in interstitial habitats of low-order rural streams with different bedrock geology. *Archiv für Hydrobiologie*, 164(2), pp.169–191. Available at: http://www.ingentaselect.com/rpsv/cgi-bin/cgi?ini=xref&body=linker&reqdoi=10.1127/0003-9136/2005/0164-0169 [Accessed November 27, 2012].

Lewis, W.M., Wurtsbaugh, W.A. & Paerl, H.W., 2011. Rationale for control of anthropogenic nitrogen and phosphorus to reduce eutrophication of inland waters. *Environmental Science & Technology*, 45, pp.10300–10305. Available at: <Go to ISI>://WOS:000298118300008.

Madigan, M.T. et al., 2009. *Brock Biology of Microorganisms* 12th ed. G. Carlson & L. Berriman, eds., San Francisco, California: Pearson Education, Inc.

Mahne, I. & Tiedje, J.M., 1995. Criteria and methodology for identifying respiratory denitrifiers. *Applied and Environmental Microbiology*, 61, pp.1110–1115. Available at: <Go to ISI>://WOS:A1995QJ88900041.

McCrackin, M.L. & Elser, J.J., 2010. Atmospheric nitrogen deposition influences denitrification and nitrous oxide production in lakes. *Ecology*, 91, pp.528–539 ST – Atmospheric nitrogen deposition infl. Available at: <Go to ISI>://WOS:000275816900024.

Minnesota Department of Natural Resources (MDNR), 2012. Habitat preservation projects easement and management areas: Eagle Creek Aquatic Management Area. Available at: http://www.dnr.state.mn.us/eco/nongame/land_preservation/projects.html.

Minnesota Pollution Control Agency (MPCA), 2012. TMDL Project: Bluff Creek TMDL — Turbidity and Fish Biota. Available at: http://www.pca.state.mn.us/index.php/water/water-types-and-programs/minnesotas-impaired-waters-and-tmdls/tmdl-projects/minnesota-river-basin-tmdl/project-bluff-creek-turbidity-and-fish-biota.html.

Mosier, A.C. & Francis, C.A., 2010. Denitrifier abundance and activity across the San Francisco Bay estuary. *Environmental Microbiology Reports*, 2(5), pp.667–676. Available at: http://doi.wiley.com/10.1111/j.1758-2229.2010.00156.x [Accessed November 29, 2012].

Mulholland, P J et al., 2009. Nitrate removal in stream ecosystems measured by (15)N addition experiments: Denitrification. *Limnology and Oceanography*, 54(3), pp.666–680. Available at: <Go to ISI>://WOS:000268325000002.

Mulholland, P J et al., 2008. Stream denitrification across biomes and its response to anthropogenic nitrate loading. *Nature*, 452, pp.202–5. Available at: http://www.ncbi.nlm.nih.gov/pubmed/18337819 [Accessed July 14, 2012].

Mulholland, P. J. et al., 2000. Nitrogen cycling in a forest stream determined by a 15N tracer addition. *Ecological Monographs*, 70(3), pp.471–493.

Nangia, V., Gowda, P.H. & Mulla, D.J., 2010. Effects of changes in N-fertilizer management on water quality trends at the watershed scale. *Agricultural Water Management*, 97(11), pp.1855–1860. Available at: http://linkinghub.elsevier.com/retrieve/pii/S0378377410002301 [Accessed October 2, 2012].

Newbold, J.D. et al., 1981. Measuring nutrient spiralling in streams. *Canadian Journal of Fisheries and Aquatic Sciences*, 38, pp.860–3. Available at: <Go to ISI>://WOS:A1981MF01200015.

Otani, Y., Hasegawa, K. & Hanaki, K., 2004. Comparison of aerobic denitrifying activity among three cultural species with various carbon sources. *Water Science and Technology*, 50(8), pp.15–22.

O'Brien, J.M. et al., 2012. The fate of assimilated nitrogen in streams: an in situ benthic chamber study. *Freshwater Biology*, 57(6), pp.1113–1125. Available at: http://doi.wiley.com/10.1111/j.1365-2427.2012.02770.x [Accessed November 28, 2012].

O'Connor, B.L. & Hondzo, M., 2008. Enhancement and inhihition of denitrification by fluid-flow and dissolved oxygen flux to stream sediments. *Environmental Science & Technology*, 42, pp.119–125. Available at: <Go to ISI>://000252037400022.

O'Connor, B.L., Hondzo, M. & Harvey, J.W., 2010. Predictive modeling of transient storage and nutrient uptake: implications for stream restoration. *Journal of Hydraulic Engineering-ASCE*, 136, pp.1018–1032. Available at: <Go to ISI>://WOS:000284276300006.

Parsheh, M., Sotiropoulos, F. & Porte-Agel, F., 2010. Estimation of power spectra of acoustic-doppler velocimetry data contaminated with intermittent spikes. *Journal of Hydraulic Engineering-Asce*, 136, pp.368–378. Available at: <Go to ISI>://WOS:000277742500004.

Patureau, D. et al., 2000. Aerobic denitrifiers isolated from diverse natural and managed ecosystems. *Microbial Ecology*, 39, pp.145–152. Available at: <Go to ISI>://000087333300005.

Peterson, B.J. et al., 2001. Control of nitrogen export from watersheds by headwater streams. *Science*, 292(5514), pp.86–90. Available at: http://www.ncbi.nlm.nih.gov/pubmed/11292868 [Accessed July 14, 2012].

Pina-Ochoa, E. et al., 2006. Denitrification in aquatic environments: A cross-system analysis. *Biogeochemistry*, 81(1), pp.111–130. Available at: http://www.springerlink.com/index/10.1007/s10533-006-9033-7 [Accessed November 5, 2012].

Pinardi, M. et al., 2009. Benthic metabolism and denitrification in a river reach: a comparison between vegetated and bare sediments. *Limnology*, 68(1), pp.133–145.

Pind, A., RisgaardPetersen, N. & Revsbech, N.P., 1997. Denitrification and microphytobenthic NO3- consumption in a Danish lowland stream: diurnal and seasonal variation. *Aquatic Microbial Ecology*, 12, pp.275–284. Available at: <Go to ISI>://WOS:A1997XD13100008.

Preston, S.D. et al., 2011. Factors affecting stream nutrient loads: a synthesis of regional SPARROW model results for the continental United States. *Journal of the American Water Resources Association*, 47, pp.891–915. Available at: <Go to ISI>://WOS:000296147200002.

Riley Purgatory Bluff Creek Watershed District (RPBCWD), 2011. *Purgatory Creek, One Water*, Minneapolis, MN.

Royer, T. V, Tank, J L & David, M.B., 2004. Transport and fate of nitrate in headwater agricultural streams in Illinois. *Journal of Environmental Quality*, 33, pp.1296–1304. Available at: <Go to ISI>://WOS:000222855900013.

Runkel, R.L., 1998. One-dimensional transport with inflow and storage (OTIS): a solute transport model for streams and rivers. , p.80.

Schipper, L.A. et al., 2010. Denitrifying bioreactors - An approach for reducing nitrate loads to receiving waters. *Ecological Engineering*, 36(11), pp.1532–43. Available at: http://dx.doi.org/10.1016/j.ecoleng.2010.04.008.

Scott County Soil Water Conservation District (Scott County SWCD), 2008. Eagle Creek station watershed outlet monitoring program annual report. , p.6.

Seitzinger, S. et al., 2006. Denitrification across landscapes and waterscapes: A synthesis. *Ecological Applications*, 16(6), pp.2064–2090. Available at: <Go to ISI>://WOS:000242849300004.

Seitzinger, S.P. et al., 2002. Nitrogen retention in rivers: model development and application to watersheds in the northeastern USA. *Biogeochemistry*, 57, pp.199–237. Available at: <Go to ISI>://WOS:000176001500007.

Smith, M.S., Firestone, M.K. & Tiedje, J.M., 1978. The acetylene inhibition method for short-term measurement of soil denitrification and its evaluation using nitrogen-13. *Soil Science Society of America*, 42(4), pp.611–615.

Solomon, C.T. et al., 2009. Sediment size and nutrients regulate denitrification in a tropical stream. *Journal of the North American Benthological Society*, 28(2), pp.480–490.

Stoddard, J.L., 1994. Long-term changes in watershed retention of nitrogen. In *Advance in Chemistry Series 237*. Washington, D.C.: American Chemical Society, pp. 223–284.

Strickland, J.D.H. & Parsons, T.R., 1972. *A Practical Handbook of Seawater Analysis*, Fisheries Research Board of Canada.

Stull, R.B., 1988. *An Introduction to Boundary Layer Meteorology*, Norwell, Massachusetts: Kluwer Academic Publishers.

Thorp, J. & Delong, A., 2002. Dominance of autochthonous autotrophic carbon in food webs of rivers heterotrophic. *OIKOS*, 96(3), pp.543–550.

Thouin, J.A. et al., 2009. The biogeochemical influences of NO3, dissolved O2 , and dissolved organic C on stream NO3 uptake. *Journal of the North American Benthological Society*, 28(4), pp.894–907. Available at: http://www.bioone.org/doi/abs/10.1899/08-183.1 [Accessed November 29, 2012].

Throbäck, I.N. et al., 2004. Reassessing PCR primers targeting nirS, nirK and nosZ genes for community surveys of denitrifying bacteria with DGGE. *FEMS microbiology ecology*, 49(3), pp.401–17. Available at: http://www.ncbi.nlm.nih.gov/pubmed/19712290 [Accessed October 26, 2012].

Tiedje, J.M., Simkins, S. & Groffman, P.M., 1989. Perspectives on measurements of denitrification in the field including recommended protocols for acetylene based methods. *Plant and Soil*, 115, pp.261–284. Available at: <Go to ISI>://WOS:A1989AG59200011.

Townsend, A.R. & Howarth, R.W., 2010. Fixing the global nitrogen problem. *Scientific American*, 302, pp.64–71.

Töwe, S. et al., 2010. Abundance of microbes involved in nitrogen transformation in the rhizosphere of Leucanthemopsis alpina (L.) Heywood grown in soils from different sites of the Damma glacier forefield. *Microbial ecology*, 60(4), pp.762–70. Available at: http://www.ncbi.nlm.nih.gov/pubmed/20549199 [Accessed November 23, 2012].

Wakelin, S.A. et al., 2011. Bacterial community structure and denitrifier (nir-gene) abundance in soil water and groundwater beneath agricultural land in tropical North Queensland, Australia. *Soil Research*, 49(1), pp.65–76. Available at: <Go to ISI>://WOS:000286945800006.

Warneke, S. et al., 2011. Nitrate removal, communities of denitrifiers and adverse effects in different carbon substrates for use in denitrification beds. *Water Research*, 45, pp.5463–5475. Available at: <Go to ISI>://WOS:000295894600012.

Watson, C.J., Jordan, C. & Allen, M.D.B., 1994. Relationships between denitrifying enzyme activity and soil properties. *Biology and Environment: Proceedings of the Royal Irsh Academy*, 94(3), pp.237–244.

7 Appendix

Derivation of Dimensionless Groups

Dimensional analysis was performed in an attempt to simplify the often complex relationship of the variables governing denitrification in stream systems:

$$J_{NO_3} = f\left(C_{NO_3}, H, u_*, \upsilon, BOM, \rho_B\right)$$

where J_{NO_3} is the denitrification potential of stream sediments based on denitrification enzyme assays, C_{NO_3} is the vertically-averaged NO_3 concentration in the water column, H is the stream depth, u_* is the shear velocity as measured using velocity fluctuations, υ is the kinematic viscosity, BOM is the Benthic Organic Matter and ρ_B is the bulk density of the sediment. Within these seven variables are 3 distinct units: milligrams, meters and seconds. According to Buckingham's pi-theorem, 4 nondimensional groups are needed to describe 7 independent variables with 3 primary dimensions (Buckingham 1914). Using Buckingham's pi-theorem, repeating parameters were chosen to be C_{NO_3}, H and u_*, which include all primary dimensions. Utilizing these repeating parameters our dimensionless groups can be chosen as

$$\Pi_1 = \Pi_1\left(J_{NO_3}, C_{NO_3}, H, u_*\right)$$

$$\Pi_2 = \Pi_2\left(BOM, C_{NO_3}, H, u_*\right)$$

$$\Pi_3 = \Pi_3\left(\rho_B, C_{NO_3}, H, u_*\right)$$

$$\Pi_4 = \Pi_4\left(\upsilon, C_{NO_3}, H, u_*\right)$$

For Π_1 we can write,

$$\left[J_{NO_3}\right]\left[C_{NO_3}\right]^{\alpha}\left[u_*\right]^{\beta}\left[H\right]^{\gamma} = L^0t^0M^0$$

where L, t and M represent the primary dimensions of meters, seconds and milligrams, respectively. The units for J_{NO_3}, C_{NO_3}, u_* and H can be expressed in these dimension as

$$\left[\frac{M}{L^2t}\right]\left[\frac{M}{L^3}\right]^{\alpha}\left[\frac{L}{t}\right]^{\beta}\left[L\right]^{\gamma} = L^0t^0M^0$$

Collecting terms for each fundamental dimension

For $M: 1+\alpha = 0$

For $t: -1-\beta = 0$

For $L: -2-3\alpha+\beta+\gamma = 0$

Solving for M and t we get $\alpha = -1, \beta = -1$. Inserting these equalities and solving for L we get $-2-3(-1)+(-1)+\gamma = 0$, or $\gamma = 0$.

The first nondimensional group is thus

$$\Pi_1 = \left[\frac{J_{NO_3}}{u_*C_{NO_3}}\right]$$

For the second nondimensional group, Π_2, we can write

$$\left[BOM\right]\left[C_{NO_3}\right]^{\alpha}\left[u_*\right]^{\beta}\left[H\right]^{\gamma} = L^0t^0M^0$$

where BOM has dimensions M L^{-2}, therefore

$$\left[\frac{M}{L^2}\right]\left[\frac{M}{L^3}\right]^{\alpha}\left[\frac{L}{t}\right]^{\beta}[L]^{\gamma} = L^0 t^0 M^0$$

Collecting terms for each fundamental dimension

For $M: 1+\alpha = 0$

For $t: -\beta = 0$

For $L: -2-3\alpha+\beta+\gamma = 0$

Solving for M and t we get $\alpha = -1$, $\beta = 0$. Inserting these equalities and solving for L we get

$-2-3(-1)+(0)+\gamma = 0$ or $\gamma = 1$.

The second nondimensional group is thus

$$\Pi_2 = \left[\frac{BOM}{HC_{NO_3}}\right]$$

For the third nondimensional group, Π_3, we can write,

$$[\rho_B]\left[C_{NO_3}\right]^{\alpha}[u_*]^{\beta}[H]^{\gamma} = L^0 t^0 M^0$$

where ρ_B has dimensions M L^{-3}, therefore

$$\left[\frac{M}{L^3}\right]\left[\frac{M}{L^3}\right]^{\alpha}\left[\frac{L}{t}\right]^{\beta}[L]^{\gamma} = L^0 t^0 M^0$$

Collecting terms for each fundamental dimension

For $M: 1+\alpha = 0$

For $t: -\beta = 0$

For $L: -3-3\alpha+\beta+\gamma = 0$

Solving for M and t we get $\alpha = -1$, $\beta = 0$. Inserting these equalities and solving for L we get

$-3-3(-1)+(0)+\gamma = 0$ or $\gamma = 0$.

The third nondimensional group is thus

$$\Pi_3 = \left[\frac{\rho_B}{C_{NO_3}}\right]$$

Lastly, for the fourth nondimensional group, Π_4, we can write,

$$[\upsilon]\left[C_{NO_3}\right]^{\alpha}[u_*]^{\beta}[H]^{\gamma} = L^0t^0M^0$$

where υ has dimensions $L^2\ t^{-1}$, therefore

$$\left[\frac{L^2}{t}\right]\left[\frac{M}{L^3}\right]^{\alpha}\left[\frac{L}{t}\right]^{\beta}[L]^{\gamma} = L^0t^0M^0$$

Collecting terms for each fundamental dimension

For $M: \alpha = 0$

For $t: -1-\beta = 0$

For $L: 2-3\alpha+\beta+\gamma = 0$

Solving for M and t we get $\alpha = 0$, $\beta = -1$. Inserting these equalities and solving for L we get

$2-3(0)+(-1)+\gamma=0$ or $\gamma=-1$.

The third nondimensional group then is

$$\Pi_4=\left[\frac{\upsilon}{u_* H}\right]=\left[\frac{1}{Re_*}\right]$$

As Re_* is already dimensionless this can be inverted to read

$$\Pi_4=\left[Re_*\right]$$

Combing dimensionless terms and introducing exponents a, b and c (which are solved for as stated in chapter 3) we get

$$\left\langle\frac{J_{NO_3}}{u_* C_{NO_3}}\right\rangle=f\left[\left\langle Re_*\right\rangle^a\left\langle\frac{BOM}{HC_{NO_3}}\right\rangle^b\left\langle\frac{\rho_B}{C_{NO_3}}\right\rangle^c\right]$$